Journal Pre-proofs

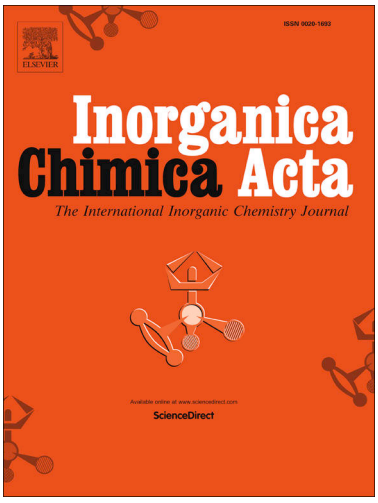

Research paper

Three new dinuclear nickel(II) complexes with amine pendant-armed ligands: characterization, DFT study, antibacterial and hydrolase-like activity

Cláudia C.V. Chaves, Giliandro Farias, Maíra D. Formagio, Ademir Neves, Rosane M. Peralta, Jane M.G. Mikcha, Bernardo de Souza, Rosely A. Peralta

PII: S0020-1693(20)30153-5
DOI: https://doi.org/10.1016/j.ica.2020.119559
Reference: ICA 119559

To appear in: *Inorganica Chimica Acta*

Received Date: 27 January 2020
Revised Date: 25 February 2020
Accepted Date: 27 February 2020

Please cite this article as: C.C.V. Chaves, G. Farias, M.D. Formagio, A. Neves, R.M. Peralta, J.M.G. Mikcha, B. de Souza, R.A. Peralta, Three new dinuclear nickel(II) complexes with amine pendant-armed ligands: characterization, DFT study, antibacterial and hydrolase-like activity, *Inorganica Chimica Acta* (2020), doi: https://doi.org/10.1016/j.ica.2020.119559

Three new dinuclear nickel(II) complexes with amine pendant-armed ligands: characterization, DFT study, antibacterial and hydrolase-like activity

Cláudia C. V. Chaves[a], Giliandro Farias[a], Maíra D. Formagio[c], Ademir Neves[a], Rosane M. Peralta,[b,] Jane M. G. Mikcha[c], Bernardo de Souza[a], Rosely A. Peralta[a]*

[a]Departamento de Química, Universidade Federal de Santa Catarina, Florianópolis, Santa Catarina, 88040-900, Brazil

[b]Departamento de Bioquímica, Universidade Estadual de Maringá, Maringá, Paraná, 87015-900, Brazil

[c]Departamento de Análises Clínicas e Biomedicina, Universidade Estadual de Maringá, Maringá, Paraná, 87020-900, Brasil

Corresponding author: Rosely A. Peralta
email:rosely.peralta@ufsc.br

KEYWORDS: Dinuclear Ni(II) complexes, hydrolase, second coordination sphere, antibacterial activity

ABSTRACT: Herein, we report the synthesis and characterization of three new Ni(II) complexes, namely: $[Ni_2(H_2LEt)(\mu\text{-}OAc)_2(H_2O)]BPh_4{\cdot}ClO_4$ (**1**), (H_2LEt = 2-[(*N*-benzyl-*N*-2-pyridyl methylamine)]-4-methyl-6-[*N*-2(pyridylmethyl)aminomethyl)]-6((2-aminoethyl)amino)methyl phenol); $[Ni_2(H_2LProp)(\mu\text{-}OAc)_2(H_2O)](ClO_4)_2$ (**2**), (H_2LProp = 2-[(*N*-benzyl-*N*-2-pyridylmethylamine)]-4-methyl-6-[*N*-(2-pyridylmethyl)aminomethyl]-6-((2-aminopropyl) amino)methylphenol); and $[Ni_2(LBut)(\mu\text{-}OAc)_2(H_2O)](HCl)_2$ (**3**), (LBut = 2-[(*N*-benzyl-*N*-2-pyridylmethylamine)]-4-methyl-6-[*N*-(2-pyridylmethyl)aminomethyl]-6-((2-aminobuthyl) amino)methylphenol). All of them were characterized through spectroscopic techniques (elemental analysis, IR, UV-Vis spectroscopy), ESI-MS, electrochemistry and potentiometric titration. Density functional theory (DFT) was used to better understand the electronic and

molecular structure of these complexes. The hydrolytic activity of complexes **1** – **3** towards the 2,4-BDNPP substrate was analyzed and complex **2** presented the highest catalytic efficiency (k_{cat}/K_M) of the three, possibly due to a greater interaction with the substrate. The complexes were also screened for their antibacterial activities using both Gram-positive and Gram-negative bacterial strains by minimum inhibitory concentration and minimum bactericidal concentration methods.

Abbreviations

2,4-DNPP	2,4-dinitrophenylphosphate
2,4-DNP	2,4-dinitrophenolate
CHES	*N*-cyclohexyl-2-aminoethanesulfonic acid
DNA	Deoxyribonucleic acid
H_2BPPAMFF	2-[(*N*-benzyl-*N*-2-pyridylmethyl-amine)]-4-methyl-6-[*N*-(2-pyridylmethyl)aminomethyl]-4-methyl-6-formylphenol
HEPES	2-[4-(2-hydroxyethyl)-piperazin-1-yl]ethanesulfonic acid
MES	2-(*N*-morpholino)ethanesulfonic acid
TD-DFT/TDA	Time-dependent-density functional theory/Tamm-Dancoff approximation
TS	Transition state

1. Introduction

Hydrolases are well-known enzymes that are of considerable interest due to their ability to make use of water molecules to promote the cleavage of chemical bonds. This feature plays a crucial role in organisms, in which some enzymes are able to cleave the DNA in a hydrolytic fashion [1-3]. The half-life of a phosphodiester bond in DNA has been estimated to be hundreds to thousands of millions of years [4], which explains why phosphate esters are so resistant toward hydrolysis under physiological conditions.

Phosphatases are enzymes that hydrolytically cleave phosphoester bonds in particular, playing an important role in cellular regulation and signaling and they are among the most extensively studied

metalloenzymes [5,6]. Therefore, over the past few decades a series of model complexes able to mimic their ability to cleave P-O bonds have been described in the literature [7-15]. Most of these complexes target the properties and catalytic functions of phosphatases to develop possible therapeutic drugs that could act as anticancer, antiviral and/or antibiotic agents. The design of some of these compounds has, as a common feature, the presence of a dinuclear active site, in which both metal centers play important roles in substrate hydrolysis. It has been postulated that one metal ion acts as a Lewis acid, decreasing the pK_a of the coordinated water molecule, while the other activates the substrate [4,16-21]. The most commonly used metal ions include $Fe^{II/III}$, Zn^{II}, Cu^{II}, Mn^{II} and Ni^{II} [22-30].

Although Ni^{II} complexes are mostly used to mimic ureases in the literature, some of them reportedly show significant phosphodiesterase activity [5,37-41], including that reported by Greatti *et al*. The authors describe a $Ni^{II}Ni^{II}$ complex with an unsymmetrical ligand containing an imidazole moiety, able to catalyze the hydrolysis of the bis-(2,4-dinitrophenyl)phosphate (2,4-BDNPP) substrate almost one million times faster than the noncatalyzed reaction [42]. A similar study was reported by Piovezan *et al*, in which the $Ni^{II}Ni^{II}$ complex had an unsymmetrical ligand in its structure, with an aldehyde moiety that was used to attach the complex to silica surfaces, as can be seen in Chart 1. The complex attached to silica was able to catalyze the hydrolysis of 2,4-BDNPP over a hundred thousand times faster than the noncatalyzed reaction [43]. This is an example of the role of the second coordination sphere in the catalysis. Therefore, since the so-called first sphere of coordination has been previously studied by several research groups and for a large number of metalloenzymes and their biomimetics [44-50], a new quest began in order to understand the role of the amino acid residues surrounding the active site of the metalloenzymes. These amino acid residues are called the second coordination sphere, and some authors have reported the impact that changes in their structure have on the catalytic activity of the metalloenzymes [51-59]. As for example, in the work reported by Hadler *et al*, on their studies with glycerophosphodiesterase (GpdQ), an enzyme capable to hydrolyze P–O bond of tri-, di- and monoesters, the replacement of the amino acid residue Asn80 by alanine leads to an increase in reactivity, but at the cost of decreased in affinity with the substrate if compared with the original enzyme [60]. The amino acid residues surrounding the active site of metalloenzymes can not only help to bind and activate the substrate, but also enhance the nucleophilicity of the metal-bound hydroxo groups, stabilize the charged transition state and assist the departure of the leaving group

through hydrogen-bonds or electrostatic interactions [5,54-56]. Some researchers have focused their attention on the investigation of the effects of the second coordination sphere, employing ammonium, guanidine or amido groups in the vicinity of the metal center of model complexes in order to mimic the hydrogen-bonds and/or electrostatic interactions [54]. One example of this type of study was reported by Silva and co-workers [61], who synthesized three $Fe^{III}Zn^{II}$ complexes, one of which presented an aldehyde moiety, while its derivative presented a diamine group. The complex containing the diamine group presented a k_{cat} value 3.2 times greater than the complex containing the aldehyde moiety and had a k_{cat}/K_M value 7.0 times greater than its precursor. The authors explained this through electrostatic interactions arising from the protonation of the primary amine group, which could lead to a greater affinity to the substrate.

In addition to presenting higher catalytic activity in the hydrolysis of phosphodiester substrates in comparison to other common metallic centers, such as Zn^{II}, $Fe^{II/III}$ and Mn^{II}, nickel coordination compounds are also known to cleave the DNA of certain cancer cells [62-66]. Thus, the rational design of new ligands presenting second coordination sphere interactions can bring extra insights and novel approaches for cancer treatment. Nickel compounds can also penetrate the microbial cells, inactivating their enzymes [67] and acting as antimicrobial compounds. Several authors [68-75] already reported Ni(II) complexes presenting antimicrobial activity, which is dependent on the chelate ring geometry and stability of the metal complexes. Therefore, the study of the antimicrobial effect of nickel complexes on Gram-positive and Gram-negative bacteria is of great interest, but the investigation of this subject remains insufficient.

In the aforementioned study, Piovezan and co-workers reported the synthesis of a dinuclear ligand containing an aldehyde moiety (Chart 1), which can be functionalized with side chain groups [43]. This approach could evidently be applied to the study of the second coordination sphere effects, and the insertion of amino groups in the side chain could, for example, lead to a greater interaction with the substrate. With that in mind, modifications on the ligand H_2BPPAMFF were performed by inserting aliphatic diamines in the backbone of the ligand, providing the new H_2LEt, H_2LProp and H_2LBut ligands (Chart 2). Amine groups tend to be in their positively-charged ammonium forms in solution around the pH range of hydrolytic catalytic activity, which can attract the anionic substrate 2,4-BDNPP with electrostatic contributions [76].

Considering these results and given the lack of studies focused on Ni(II) complexes presenting phosphodiesterase activity in the literature, herein we report the synthesis and characterization of

three new nickel compounds. Antibacterial studies were carried out with these compounds to determine their action against bacterial strains of *Escherichia coli*, *Salmonella typhi*, *Pseudomonas aeruginosa*, *Aeromonas hydrophila*, *Listeria innocua* and *Staphylococcus aureus* and their hydrolase-like activity towards the model substrate 2,4-BDNPP was also investigated.

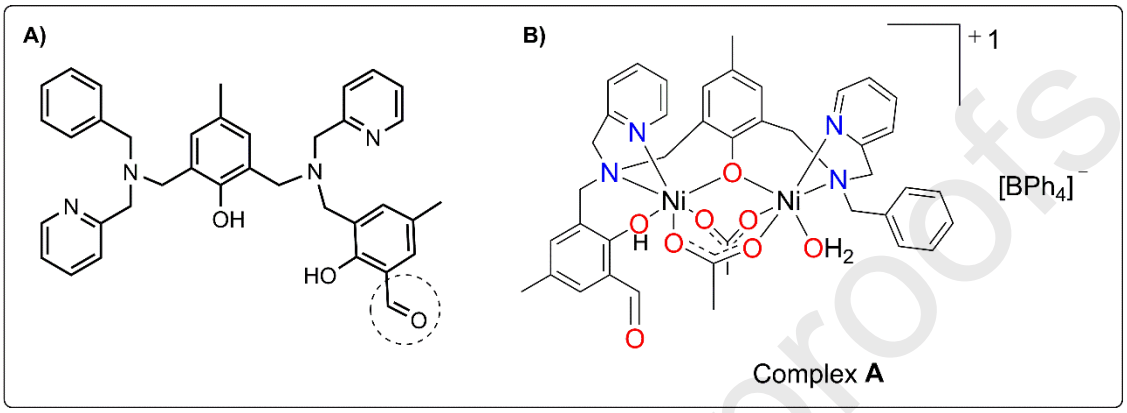

Chart 1 A) Ligand H_2BPPAMFF and B) Complex **A** reported by Piovezan *et al* [43].

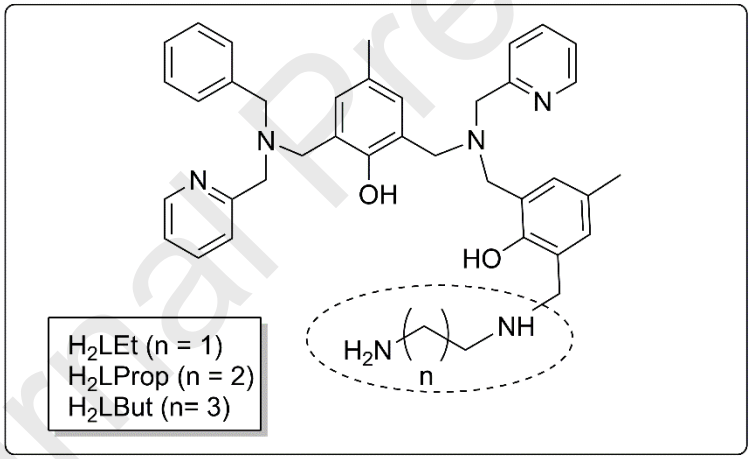

Chart 2 Ligands used in this study.

2. Experimental

2.1 *Chemicals*

The reagents, materials, gases and solvents of high purity grade used in the synthesis procedures were purchased from commercial sources and used without further purification. The 3-(chloromethyl)-2-hydroxy-5-methylbenzaldehyde [77], bis-(2,4-dinitrophenyl)phosphate [78] and the ligand 2-[(*N*-benzyl-*N*-2-pyridylmethylamine)]-4-methyl-6-[*N*-(2-

pyridylmethyl)aminomethyl]-4-methyl-6-formylphenol (H_2BPPAMFF) [43] were synthesized by previously described methods.

2.2 *Physical measurements*

Infrared spectra were obtained on a PerkinElmer Fourier transformed infrared-attenuated total reflectance (FTIR-ATR) spectrophotometer (model Spectrum 100), using a ZnSe (45º) crystal, and a triglycine sulfate (TGS) detector. The samples were analyzed directly by ATR, in the range of 4000-550 cm^{-1}, and were corrected by a blank measurement. The elemental analysis of all complexes and ligands was carried out with a CE Instruments C, H, N, S, O analyzer (model EA 1110 CHNS-O). The mass spectra for all ligands and complexes were obtained on an Amazon-ion trap mass spectrometer via electrospray ionization (ESI-MS). High-resolution mass spectra were obtained on a Bruker Daltonics spectrometer (model Q-micrOTOF Q-II) equipped with a KD Scientific automatic syringe for sample injection. The ESI-MS analysis of both ligands and complexes was carried out in an ultrapure acetonitrile solution at a concentration of 500 ppb at 180 μL min^{-1}. The capillary temperature was maintained at 180 to 200 °C and the voltage at -400 to -500 V. The simulated spectra were calculated using the Mmass software [79]. Nuclear magnetic resonance spectra (^{1}H NMR) were recorded with a Bruker FT 200 MHz instrument at room temperature and the chemical shifts were recorded in ppm using tetramethylsilane (TMS) as the internal reference (TMS, δ = 0.00 ppm) and deuterated chloroform as the solvent. Electronic spectra were obtained on a Perkin-Elmer Lambda-750 spectrophotometer in the range of 250-800 nm in acetonitrile solution. The redox behavior of the complexes was investigated by cyclic and square-wave voltammetry on a BAS potentiostat/galvanostat (model Epsilon), and the experiments were performed in acetonitrile solution under argon atmosphere. In these experiments, tetrabutylammonium hexafluorophosphate [NBu_4](PF_6) (0.1 mol L^{-1}) was used as the supporting electrolyte and measurements were taken in an electrolytic cell with three electrodes: glassy carbon (working); platinum wire (counter); and Ag/Ag^+ (reference). Ferrocene (E° = 0.4 V *vs* NHE) was used as the internal standard [80]. The Ni determination was carried out by atomic absorption spectrometry with a continuous source high resolution atomic absorption spectrometer, model ContrAA 700 (Analytik Jena, Jena, Germany), coupled with a graphite furnace and flame atomizers. The selected wavelength was 232.003 nm. A mixture of air (oxidant) and acetylene (fuel) was used with a continuous flow of 55 L h^{-1}. The burner height was fixed at 6 mm.

2.3 *Potentiometric titrations*

The potentiometric studies were carried out with a Methrom 848 Titrino Plus automatic titrator fitted with a combination electrode (Ag/AgCl) calibrated to read -log[H^+] directly, designated as the pH. The experiment temperature was maintained at 25.00±0.05 °C and gas-free deionized water was used to prepare the solutions. The ionic strength was kept constant at 0.1 mol L^{-1} through the addition of KCl. Experiments were performed in 50 mL of a CH_3CN/H_2O 1:1 (pK_w =15.40 [81]) solvent system, containing 0.025 mmol of the complex, purged with Ar, cleaned using two bubbling towers with 0.10 mol L^{-1} KOH solutions and titrated with 0.10 mol L^{-1} standard CO_2-free KOH from pH 3.00 to 12.00 through the addition of 0.025 mL aliquots of base. The experiments were run in duplicate for complex **1** and in triplicate for complexes **2** and **3**. Data analysis was performed using the BEST7 program [82] and the species diagrams were obtained with the SPE [82] and SPEPLOT [82] programs.

2.4 *Kinetic assays*

The phosphodiesterase-like activity of the complexes was determined by monitoring the hydrolysis of the substrate bis-(2,4-dinitrophenyl)phosphate (2,4-BDNPP) under substrate excess. The experiments were carried out in triplicate using a UV-Vis Varian Cary 50 BIO spectrometer at 400 nm in an CH_3CN/H_2O (1:1, v/v) mixture. The initial rates were measured in real time at various pH values between 5.00 and 9.50 (buffers used were 0.10 mol L^{-1} MES, pH 5.00-6.50, HEPES, pH 7.00-8.50 and CHES, pH 9.00-9.50) with ionic strength I = 0.10 mol L^{-1}, $LiClO_4$. The molar absorption coefficient of the product 2,4-dinitrophenolate was determined at each pH under the same experimental conditions applied to obtain the rate measurements [83]. The reactions were monitored to less than 5% of conversion. The pH dependence of the rate was investigated using fixed concentrations of the substrate ($[S]_{final}$ = 5.33 × 10^{-3} mol L^{-1} for **1**, $[S]_{final}$ = 3.33 × 10^{-4} mol L^{-1} for **2** and $[S]_{final}$ = 6.66 × 10^{-4} mol L^{-1} for **3**) and complexes ($[C]_{final}$ = 1.00 × 10^{-4} mol L^{-1} for **1**, $[C]_{final}$ = 3.33 × 10^{-6} mol L^{-1} for **2** and $[C]_{final}$ = 1.00 × 10^{-5} mol L^{-1} for **3**) at 25.0 ± 0.5 °C. Substrate dependence ($[S]_{final}$ = 2.00 × 10^{-4} mol L^{-1} – 4.40 × 10^{-3} mol L^{-1}) was measured in the pH range of 5.00 to 9.50. The data were treated using the Michaelis-Menten equation by non-linear regression [84]. In order to establish the number of molecules of substrate which are hydrolyzed per molecule of complex, the reaction was monitored at 445 nm (ε = 3600 L mol^{-1} cm^{-1}) [83], under a 50-fold

substrate excess ($[S]_{final} = 2\times10^{-4}$ mol L^{-1} for **1** and **2** and $[S]_{final} = 3\times10^{-4}$ mol L^{-1} for **3**) relative to the complex ($[C]_{final} = 4\times10^{-6}$ mol L^{-1} for **1** and **2** and $[C]_{final} = 6\times10^{-6}$ mol L^{-1} for **3**), at pH 9.00 and 25 °C. Also, a stoichiometric reaction between complexes **1**, **2** and **3** and the 2,4-BDNPP substrate (1×10^{-5} mol L^{-1}) was monitored (400 nm) at pH 9.00 and 25 °C. Isotopic effects regarding the hydrolysis rate of 2,4-BDNPP promoted by the complexes were investigated by monitoring the reactions in deuterated buffer. The effect of temperature on the reaction rates was investigated in the range 20 – 40 °C, at pH 9.00, for all complexes under the same conditions as those used to assess the substrate dependence. The studies were corrected for spontaneous hydrolysis by direct difference between two identical parallel reactions.

2.5 *Biological Studies*

The antibacterial activity of the complexes was studied by agar selective and differential methods at pH 7.2, using six strains of bacteria (*Escherichia coli*, *Salmonella typhimurium*, *Pseudomonas aeruginosa*, *Aeromonas hydrophila*, *Listeria innocua* and *Staphylococcus aureus*) by the minimum inhibitory concentration method. The different bacterial cultures were maintained in trypic soy broth (TBS, Difco, Le Pont-de-Claix, France) supplemented with 20% glycerol at -20 °C. An aliquot of the culture was seeded in brain heart infusion broth (BHI, Difco,Le Pont-de-Claix, France) and incubated for 24 h at 35 °C with exception of *S. aureus*, which was incubated for 48 h.

2.5.1 Minimum inhibitory and bactericidal concentrations

The minimum inhibitory concentration (MIC) and minimum bactericidal concentration (MBC) were determined using the 96-well microplate microdilution technique (TTP, Trasadingen, Switzerland) according to the Clinical and Laboratory Standards Institute [85]. The compounds were diluted in Mueller Hinton broth (MHB, Difco, Le Pont-de-Claix, France) in 2% acetonitrile at the final concentration and added to the microplates in batches ranging from 0.97 to 1000 µg mL^{-1}.

The bacterial cultures cultivated in MHB were standardized to the McFarland scale 0.5 and diluted to obtain 5×10^6 colony-forming units (CFU) mL^{-1} and 10 µL were inoculated in each microplate well and incubated at 35 °C for 24 h. The MIC was defined as the lowest concentration that inhibited bacterial growth by visual reading. From the wells in which the bacterial growth was not

observed, a 10 µL aliquot was inoculated in plates containing selective differential agar and incubated at 35 °C for 24 h to determine the MBC. The MBC was determined as the lowest concentration in which no bacterial growth was observed by visual inspection. The experiments were performed in triplicate.

Culture mediums were added as controls without the addition of the antimicrobial and inoculum (negative control) culture medium, with the addition of the bacterial inoculum (positive control) and control of the acetonitrile solvent (2% v/v) with the addition of the inoculum.

2.6 *Theoretical predictions*

Geometry optimizations of complexes **1**, **2** and **3** were carried out in a vacuum with the Orca 4.0.1 software package [86] at the density functional theory (DFT) level using the BP86 functional [87,88]. The basis set chosen was Def2-TZVP for the nickel atom and Def2-SVP for the other atoms [89-91]. These calculations also included Grimme's dispersion correction (D3) with Becke-Johnson damping (BJ) [92,93]. The vibrational frequencies for both complexes **1**, **2** and **3** showed no imaginary frequencies. The phosphate conjugates were also optimized, and the vibrational frequencies showed only one small negative frequency due to rotation of the aromatic rings. In order to simulate the absorption spectra, time-dependent DFT under the Tamm-Dancoff approximation (TD-DFT/TDA) was employed to obtain the first 50 excitations, using the same calculations protocol, differing only at the functional, which in this case was PBE0 [94,95], and the basis set for coordinated atoms was the same used for the nickel atom, Def2-TZVP. The 3D representations of the complexes were obtained using the Chemcraft program [96].

2.7 *Synthesis of the ligands*

Three new ligands containing side chain amino groups derived from the already known H_2BPAMFF ligand [43] were prepared.

Synthesis of 2-[(*N*-benzyl-*N*-2-pyridylmethylamine)]-4-methyl-6-[*N*-2(pyridylmethyl)aminomethyl)]-6-((2-aminoethyl)amino)methylphenol – H_2LEt. In a 500 mL round-bottom flask, 4.20 g (70 mmol; 60.10 g mol^{-1}; 0.899 g mL^{-1}) of 1,2-diaminoethane was added to 150 mL of an ethanol/dichloromethane (2:1) solution, followed by 4.10 g (7 mmol; 586.72 g mol^{-1}) of H_2BPPAMFF in 50 mL of ethanol added dropwise. The reaction mixture was left to

react overnight at room temperature. The temperature was then lowered to 0°C in an ice bath and 3.18 g (84 mmol; 37.83 g mol^{-1}) of solid sodium borohydride were added slowly, and the mixture was stirred for 2 h. The pH was adjusted to 5.0 and the solvent was removed under reduced pressure. The product was dissolved in 30 mL chloroform and washed first with a saturated sodium bicarbonate solution (2 × 15 mL), then three times with a saturated sodium chloride solution (3 × 15 mL). The organic layer was dried with anhydrous Na_2SO_4, then filtered off, and the solvent removed under reduced pressure, resulting in a pale-pink foam (yield: 93%). Anal. calcd (found) for $C_{39.5}H_{49}ClN_6O_3$: C, 68.63 (68.97); H, 7.14 (7.26); N, 12.16 (12.15). IR (ATR), in cm^{-1}: ν (C-H_{ar} and C-H_{aliph}) 3066-2712; ν (C=N and C=C) 1589-1432; δ (O-H_{phenol}) 1365; ν (C – O_{phenol}) 1228; ν (C – H_{ar}) 746-698. ^{1}H NMR - δ_H (200 MHz; $CDCl_3$), in ppm: 2.20 (s, $3H_{CH3}$); 2.21 (s, $3H_{CH3}$); 3.67 (s, $2H_{CH2}$); 2.60 – 2.66 (dt, $2H_{CH2}$); 2.75 – 2.80 (dt, $2H_{CH2}$); 3.66 (s, $2H_{CH2}$); 3.70 (s, $2H_{CH2}$); 3.74 (s, $2H_{CH2}$); 3.77 (s, $4H_{CH2}$); 3.82 (s, $2H_{CH2}$); 3.83 (s, $2H_{CH2}$); 6.81 – 6.90 (dd, $4H_{ar}$); 7.11 – 7.21 (m, $3H_{ar}$); 7.29 – 7.40 (m, $6H_{ar}$); 7.56 – 7.68 (m, $2H_{ar}$); 8.52 – 8.59 (dd, $2H_{py}$). ESI-MS: [H-$_2$LEt] + H^+, *m/z* = 631.35.

Synthesis of 2-[(*N*-benzyl-*N*-2-pyridylmethylamine)]-4-methyl-6-[*N*-(2-pyridylmethyl)aminomethyl]-6-((2-aminopropyl)amino)methylphenol – H_2LProp. In a 500 mL round-bottom flask, 5.20 g (70 mmol; 74.13 g mol^{-1}; 0.886 g mL^{-1}) of 1,3-diaminopropane was added to 150 mL of an ethanol/dichloromethane (2:1) solution, followed by 4.10 g (7 mmol; 586.72 g mol^{-1}) of H_2BPPAMFF in 50 mL of ethanol added dropwise. The reaction mixture was left to react overnight at room temperature. The temperature was lowered to 0°C in an ice bath then 3.17 g (84 mmol; 37.83 g mol^{-1}) of solid sodium borohydride were added, and the mixture was stirred for 4 h. The pH was adjusted to 5.0 and the solvent was removed under reduced pressure. The product was dissolved in 30 mL chloroform and washed first three times with a saturated sodium bicarbonate solution (3 × 15 mL), and then two times with a saturated sodium chloride solution (2 × 15 mL). The organic layer was dried with anhydrous Na_2SO_4, then filtered off, and the solvent removed under reduced pressure, resulting in a white foam (yield: 98%). Anal. calcd (found) for $C_{41}H_{52}Cl_2N_6O_3$: C, 65.85 (65.62); H, 7.01 (6.97); N, 11.24 (11.15). IR (ATR), in cm^{-1}: ν (C-H_{ar} and C-H_{aliph}) 3061-2712; ν (C=N and C=C) 1588-1433; δ (O-H_{phenol}) 1365; ν (C – O_{phenol}) 1229; ν (C – H_{ar}) 748-697. ^{1}H NMR - δ_H (200 MHz; $CDCl_3$), in ppm: 1.61 – 1.67 (q, $2H_{CH2}$); 2.21 (s, $3H_{CH3}$); 2.69 – 2.71 (t, $4H_{CH2}$); 3.66 (s, $2H_{CH2}$); 3.70 (s, $2H_{CH2}$); 3.74 (s, $2H_{CH2}$);

3.77 (s, 4H_{CH2}); 3.82 (s, 2H_{CH2}); 3.83 (s, 2H_{CH2}); 6.83 – 6.89 (dd, 4H_{ar}); 7.18 (m, 3H_{ar}); 7.29 – 7.39 (m, 6H_{ar}); 7.58 – 7.64 (m, 2H_{ar}); 8.57 (dd, 2H_{py}). ESI-MS: [H_2LProp] + H^+, *m/z* = 645.46.

Synthesis of 2-[(*N*-benzyl-*N*-2-pyridylmethylamine)]-4-methyl-6-*N*-(2-pyridylmethyl)aminomethyl-6-((2-aminobuthyl)amino)methylphenol – H_2LBut. In a 500 mL round-bottom flask, 7.052 g (80 mmol; 88.15 g mol^{-1}; 0.877 g mL^{-1}) of 1,4-diaminobuthane was added to 150 mL of an ethanol/dichloromethane (2:1) solution, followed by 4.69 g (8 mmol; 586.72 g mol^{-1}) of H_2BPPAMFF in 50 mL of ethanol added dropwise. The reaction mixture was left to react overnight at room temperature. The temperature was lowered to 0 °C in an ice bath, 3.63 g (96 mmol; 37.83 g mol^{-1}) of solid sodium borohydride were added, and the mixture was stirred for 4 h. After this time, the pH was adjusted to 5.0 and the solvent was removed under reduced pressure. The product was dissolved in 30 mL chloroform and washed first four times with a saturated sodium bicarbonate solution (4 × 15 mL), and then three times with a saturated sodium chloride solution (3 × 15 mL). The organic layer was dried with anhydrous Na_2SO_4, then filtered off, and the solvent removed under reduced pressure, resulting in a light-yellow foam (yield: 98%). Anal. calcd (found) for $C_{42}H_{56}Cl_2N_6O_4$: C, 64.69 (64.15); H, 7.24 (7.20); N, 10.78 (10.73). IR (ATR), in cm^{-1}: ν (C-H_{ar} and C-H_{aliph}) 3088-2711; ν (C=N and C=C) 1592-1432; δ (O-H_{phenol}) 1367; ν (C – O_{phenol}) 1227; ν (C – H_{ar}) 748-696. NMR - δ_H (200 MHz; $CDCl_3$), in ppm: 1.39 – 1.52 (m, 4H_{CH2}); 2.21 – 2.22 (s, 6H_{CH3}); 2.56 – 2.67 (m, 4H_{CH2}); 3.66 – 3.83 (s, 14H_{CH2}); 6.82 (s, 2H_{ar}); 6.90(s, 2H_{ar}); 7.11 – 7.21 (m, 3H_{ar}); 7.29 – 7.41 (m, 6H_{ar}); 7.55 – 7.68 (dt, 2H_{ar}); 8.52 – 8.58 (dd, 2H_{py}). ESI-MS: [H_2LBut] + H^+, *m/z* = 659.45.

2.8 *Synthesis of the Complexes*

Complexes **1**, **2** and **3** (Scheme 1) were synthesized using a procedure similar to that previously described by Piovezan *et al* [43].

Synthesis of the Complex $[Ni_2(H_2LEt)(\mu\text{-}OAc)_2(H_2O)](ClO_4)(BPh_4)$ (1). Complex (**1**) was synthesized in a (2:1) methanol/acetonitrile solution by mixing 0.37 g of $Ni(ClO_4)_2{\cdot}6H_2O$ (1 mmol; 365 g mol^{-1}) and 0.32 g of the H_2LEt ligand (0.5 mmol; 630.82 g mol^{-1}) with stirring and mild heating (55 °C). In the next step, 0.14 g of $NaCH_3COO{\cdot}3H_2O$ (1 mmol; 136.08 g mol^{-1}) and 0.17 g of $NaBPh_4$ (0.5 mmol; 342.22 g mol^{-1}) were added and a green solution was obtained. After recrystallization in a (1:1) dichloromethane/hexane solution, a green solid was obtained (yield: 0.48 g, 68%). Anal. calcd (found) for $Ni_2C_{68}H_{78}BCl_3N_6O_{12}$: C, 58.09 (57.76); H, 5.59 (5.70); N,

5.98 (6.35). IR (ATR), in cm^{-1}: ν (O – H) 3511; ν (C – H_{ar} and C – H_{alif}) 3055 – 2912; ν (C=C) 1605 – 1445; ν_{ass} (COO^-) 1554; ν_s (COO^-) 1427; ν (C – O) 1317; ν (Cl-O) 1090; δ (C-H_{ar}) 735 – 703. ESI-MS: $[Ni_2LEt(CH_3COO)]^+$, *m/z* = 803.31. Atomic absorption, in mg mL^{-1}: Ni, 2.97±0.0034.

Synthesis of the Complex $[Ni_2(H_2LProp)(\mu\text{-}OAc)_2(H_2O)](ClO_4)_2$ (2). Complex (**2**) was synthesized in a methanolic solution by mixing 0.37 g of $Ni(ClO_4)_2{\cdot}6H_2O$ (1 mmol; 365 g mol^{-1}) and 0.32 g of the H_2LProp ligand (0.5 mmol; 644.82 g mol^{-1}) with stirring and mild heating (45 °C). In the next step, 0.14 g of $NaCH_3COO{\cdot}3H_2O$ (1 mmol; 136.08 g mol^{-1}) and 0.17 g of $NaBPh_4$ (0.5 mmol; 342.22 g mol^{-1}) were added and a green solution was obtained. After recrystallization in a (1:1) ethyl acetate/acetone solution, a green solid was obtained (yield: 0.36 g, 57%). Anal. calcd (found) for $Ni_2C_{57}H_{68}B_{0.5}Cl_4N_6Na_{0.5}O_{15}$: C, 50.59 (50.68); H, 5.06 (5.08); N, 6.21 (6.20). IR (ATR), in cm^{-1}: ν (O – H) 3496; ν (C – H_{ar} e C – H_{aliph}) 3058 – 2854; ν (C=C) 1606 – 1422; ν_{ass} (COO^-) 1574; ν_s (COO^-) 1437; ν (C – O) 1318; ν (Cl-O) 1081; δ (C-H_{ar}) 759 – 703. ESI-MS: $[NiLProp(CH_3COO)]^+$, *m/z* = 877.37. Atomic absorption, in mg mL^{-1}: Ni, 2.77±0.0171.

Synthesis of the Complex $[Ni_2(LBut)(\mu\text{-}OAc)_2(H_2O)]{\cdot}(HCl)_2$ (3). Complex (**3**) was synthesized in a (2:1) methanol/acetonitrile solution by mixing 0.25 g of $Ni(OAc)_2{\cdot}4H_2O$ (1 mmol; 248.86 g mol^{-1}) and 0.33 g of the H_2LBut ligand (0.5 mmol; 658.82 g mol^{-1}) with stirring and mild heating (45 °C). In the next step, 0.34 g of $NaBPh_4$ (1 mmol; 342.22 g mol^{-1}) was added to the mixture and a green solution was obtained. The resulting green solid was collected and washed with distilled water (yield: 0.58 g, 94%). Anal. calcd. (found) for $Ni_2C_{93}H_{98}B_2Cl_2N_6Na_2O_7$: C, 66.98 (66.67); H, 5.92 (5.91); N, 5.04 (5.54). IR (ATR), in cm^{-1}: ν (C – H_{ar} and C – H_{aliph}) 3055 – 2859; ν (C=C) 1603 – 1412; ν_{ass} (COO^-) 1577; ν_s (COO^-) 1439; ν (C – O) 1315; δ (C-H_{ar}) 757 – 701. ESI-MS: $[Ni_2LBut(CH_3COO)_2(H_2O)_2(Na)_2(Cl)]^+$, *m/z* = 1007.32. Atomic absorption, in mg mL^{-1}: Ni, 3.36±0.0114.

Caution! *Perchlorate salts of metal complexes are potentially explosive.*

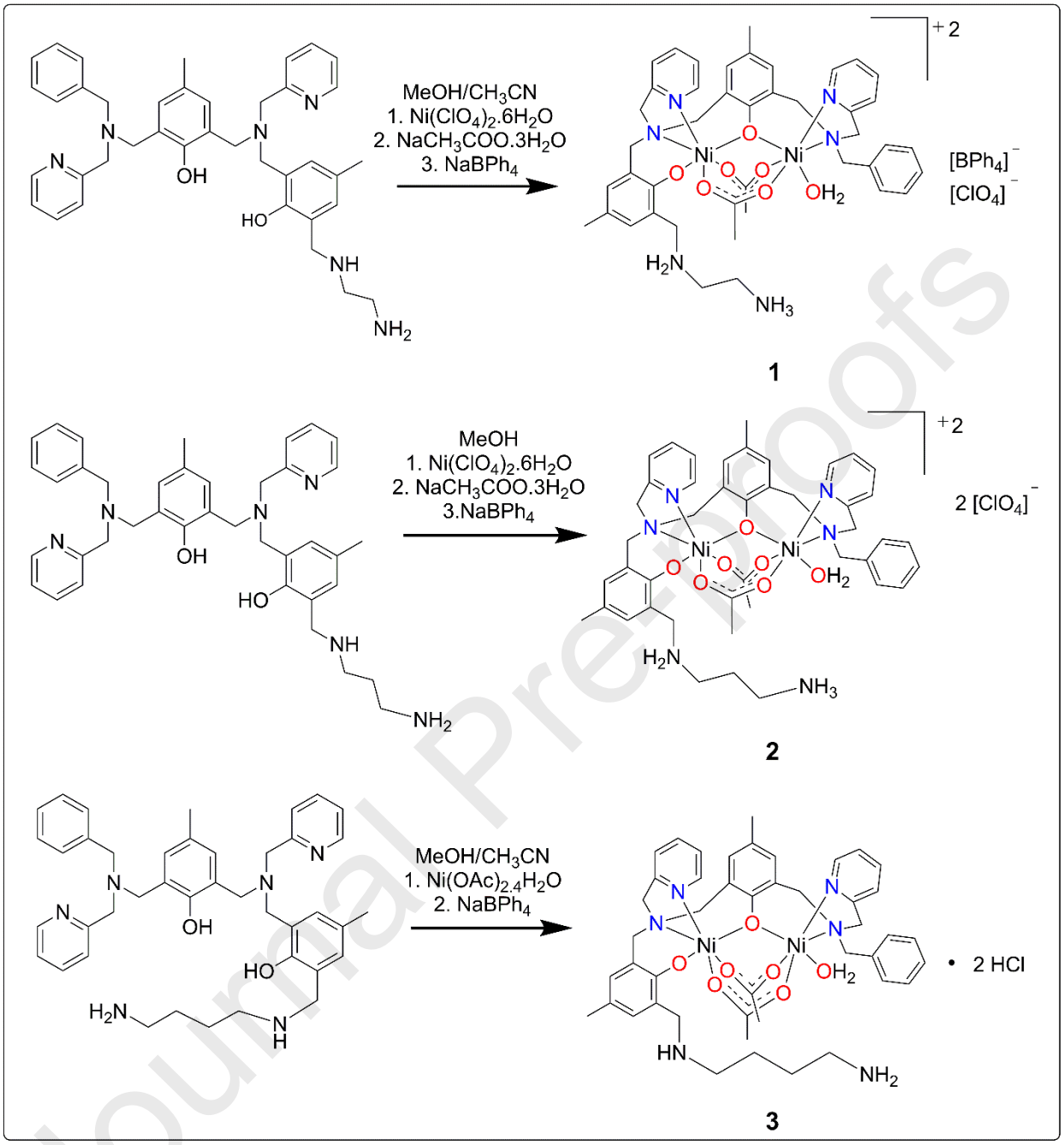

Scheme 1. Schemes showing the synthesis of complexes **1**, **2** and **3**.

3. Results and discussion

3.1 *Synthesis of the ligands and complexes*

The synthetic route to the unsymmetric ligands (H_2LEt, H_2LProp and H_2LBut) is illustrated in Figure S1. The three ligands were fully characterized by ^{1}H NMR, IR and ESI-MS techniques (Figures S26-S28). The reaction of the ligands with Ni(II) salts, as described above, afforded the complexes **1**, **2** and **3** as green solids.

3.2 *Solid-state and DFT studies*

3.2.1 Infrared (IR) spectroscopy

The IR spectra for **1**, **2** and **3** (Figures S2, S3 and S4 and Table S1) present bands of ν_{ass} (COO^-) and ν_s (COO^-) with Δ = 127 cm^{-1}, 137 cm^{-1} and 138 cm^{-1} for **1**, **2** and **3** respectively, indicating the coordination of a carboxylate group in a bridging mode [97]. Bands at 1090 cm^{-1} and 1081 cm^{-1} for **1** and **2**, respectively, related to the stretching of the Cl-O bond of the counterion were present in all spectra. The results obtained for complexes **1** – **3** agree with those reported for similar complexes in the literature [42,43], as well as the frequencies obtained in the DFT studies (*vide* SI - IR spectroscopy).

3.2.2 DFT modeling of the structures

Since no single crystals were obtained for X-ray analysis, DFT was used to predict likely structures (and also to help to understand the experimental data) for complexes **1**-**3** and their phosphate conjugates. The optimization of the structures for the three complexes was carried out only on the predominant species at the optimum kinetic pH value. The calculations were performed with a terminal hydroxo group bonded to the nickel center on the soft moiety of the ligand and a water ligand in the nickel center on the hard moiety. In agreement with the potentiometric titration studies, it was also assumed that the terminal amines of the ligands were protonated in their phosphate conjugates. Also, the spin of the Ni^{II} ion was set equal to 1 as reported by Piovezan *et al* [43]. As shown in Figure S5, all of the nickel centers exhibit a pseudo-octahedral geometry, which is expected for these complexes, based on previous studies with similar systems [43]. As can be seen in Table S2, all of the bonds and angles were in good agreement with those previously reported for Ni^{II}(μ-OH)Ni^{II} complexes for which X-ray structures were obtained [43]. The calculated vibrational frequencies and intensities were compared with the experimental infrared spectra (Figures S6-S8), showing reasonable agreement. It is important to note that no perchlorate

anion was included in the theoretical predictions; hence, the lack of the intense band at around 1100 cm^{-1}. Table S3 shows the assignments of the IR bands for complexes **1**–**3** (experimental and calculated).

3.3 *Solution studies*

3.3.1 Mass spectrometry (MS)

The ESI-MS analysis of complexes **1**, **2** and **3** was performed in a pure acetonitrile solution. The mass spectrum of complex **1** showed a group of peaks with a maximum (100%) at *m/z* 460.15 with a +2 charge, which can be assigned to the system $[Ni^{II}Ni^{II}(\mu\text{-}CH_3COO)(HLEt)]+CH_3OH+CH_2Cl_2$ (Figure S9). Another group of peaks (intensity = 28%) at *m/z* 803.31 with a +1 charge was observed and can be assigned to the $[Ni^{II}Ni^{II}(\mu\text{-}CH_3COO)(LEt)]$ species (Figure S10). For complex **2** a group of peaks with a maximum (100%) at *m/z* 817.32 and a +1 charge was observed and can be assigned to $[Ni^{II}Ni^{II}(\mu\text{-}CH_3COO)(LProp)]$ (Figure S11). The mass spectrum for complex **3** showed a group of peaks with a maximum (100%) at *m/z* 1007.32 and a +1 charge, which can be assigned to $[Ni^{II}Ni^{II}(\mu\text{-}CH_3COO)_2(HLBut)]+4H_2O+Na^{+}+Cl^{-}$ (Figure S12). Another group of peaks (29%) at *m/z* 831.36 with a +1 charge can be seen, which can be assigned to $[Ni^{II}Ni^{II}(\mu\text{-}CH_3COO)(LBut)]$ species (Figure S13).

3.3.2 Electronic absorption spectroscopy and DFT studies

The electronic spectra of **1**, **2** and **3** were investigated in the range of 250 – 800 nm in acetonitrile solution and present bands at λ_{max}, nm (ε, L mol^{-1} cm^{-1}), of 609 (14), 616 (15) and 626 (23), respectively (Figures S14-S16). These can be attributed to *d-d* transitions, showing a bathochromic shift as the side chain amino group increases in size from two to four carbon atoms. The bathochromic shift can also be observed when we compare the λ_{max} values of complex $[Ni(HBPPAMFF)(\mu OAc)_2(H_2O)]BPh_4$ (**A**), reported by Piovezan and coworkers [43] – which contains an aldehyde moiety in its structure – with those of complexes **1 – 3,** as can be seen in Table 1. A weak band is also observed at around 770 nm for all complexes and is attributed to a spin-forbidden transition. The diffuse reflectance spectra of complexes **1** – **3** exhibit bands at approximately 614 nm, 622 nm and 628 nm, respectively, as well as a weak band at around 770 nm (Figures S14-S16), indicating that the structures are maintained in solution. These values agree with those for other complexes previously described in the literature [17,27,31,39,41,42,43,62,98].

The calculated frontier orbitals for complexes **1 – 3** are shown in Figure 1. It can be observed that for all complexes the last alpha and beta occupied orbitals are spread over the substituted phenol moiety of the ligand with a slight contribution of *dπ* orbitals of the Ni(II) center, and there is no significant influence from the different lateral groups. The first unoccupied orbitals are located over the pyridine coordinated to the same nickel center, also with a small contribution of *dπ* orbitals from the Ni(II). Time-dependent DFT (TD-DFT) was used to simulate the absorption spectra and help to understand the assignments from the experimental spectra (Figures S17-19). Based on these calculations, the low energy bands (~550-900 nm) of **1-3** can be resolved in a few excitations, all of which are related to *d-d* like transitions, where donor molecular orbitals have a small contribution from the coordinated oxygen atoms and the acceptor molecular orbitals have a small contribution from the phenol moieties. The transitions involving mostly the frontier orbitals described above are located in the region between 550 and 400 nm. The remaining transitions at the high energy end of the spectrum could be assigned as *π*-*π**-like transitions with a small contribution from CT transitions involving the Ni(II) center.

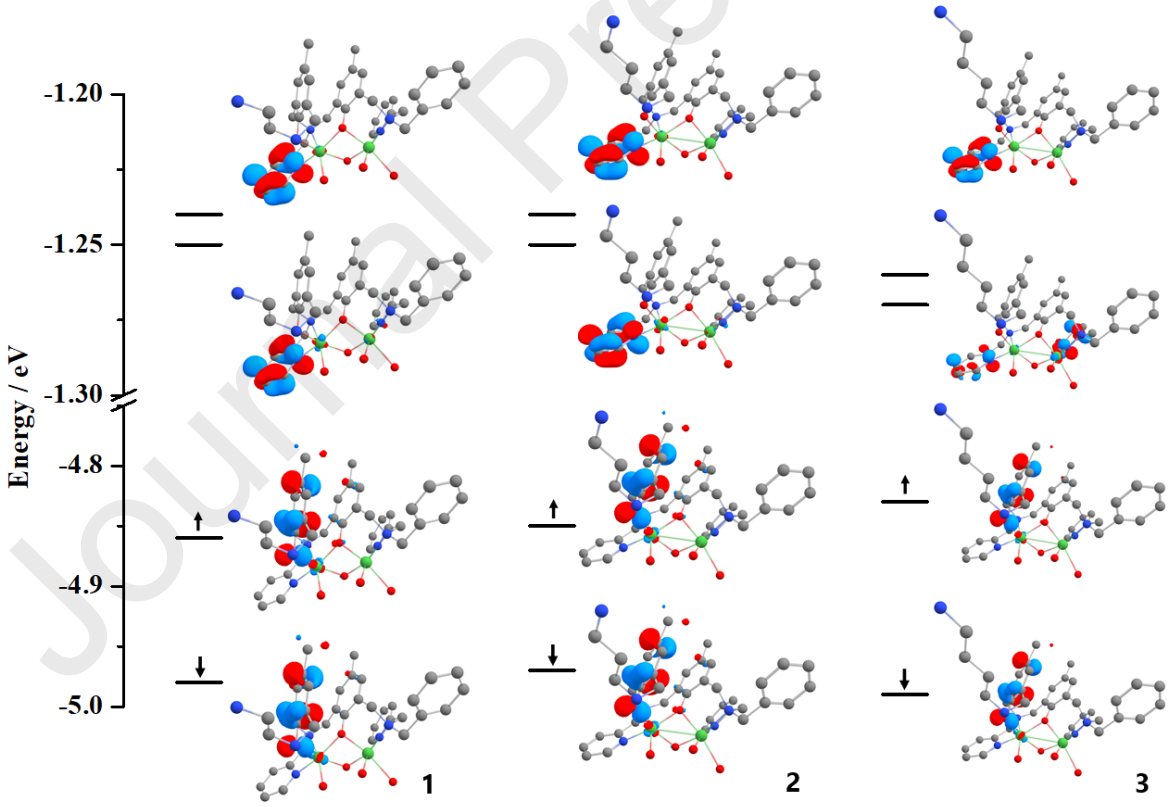

Figure 1. Calculated frontier orbitals of complexes **1**, **2** and **3**.

3.3.3 Electrochemical properties and molar conductivity

Cyclic and square-wave voltammograms were recorded in dry acetonitrile in the potential range -2.0 to +2.0 V *versus* NHE, using $[NBu_4][(PF_6)]$ as the supporting electrolyte and ferrocene as the internal standard ($E_{1/2}$ = 0.4 V *vs* NHE) [80]. In the cyclic voltammograms for complexes **1 – 3**, one irreversible wave was observed (Figures S20, S22 and S24) in the cathodic region, which can be attributed to the one-electron transfer processes $Ni^{II}Ni^{II}/Ni^{II}Ni^{I}$ while in the anodic region two waves were detected for all complexes and are attributed to the oxidation of the ligands (Figures S20, S22 and S24). However, the possibility of these processes being associated with the oxidation of the Ni(II) centers cannot be excluded. The square-wave voltammograms for complexes **1** and **3** showed a *quasi*-reversible behavior (Figures S21 and S25), which can be attributed to the one-electron transfer processes $Ni^{II}Ni^{II}/Ni^{II}Ni^{I}$ and $Ni^{II}Ni^{II}/Ni^{II}Ni^{II}$, whereas for complex **2** only one cathodic wave could be observed (Figure S23). From the values listed in Table 1 it is possible to infer an anodic shift from complex **A** [43] to **3**, which agrees with the bathochromic shift observed on the UV spectra. This can be explained by interactions related to the protonated amino group and the terminal water molecule bonded to the metal center (vide potentiometric data, section 3.4), which causes the withdrawn of electron density from the metal center, thereby favoring its reduction [17,61,99]. The measured molar conductivity of the complexes in acetonitrile solution at 25 °C was 121 S cm^2 mol^{-1} for **1**, 140 S cm^2 mol^{-1} for **2**, which is characteristic of a 1:1 electrolyte. The value of 36 S cm^2 mol^{-1} for **3** is characteristic for a neutral species in solution [100]. In addition, the atomic absorption spectrometry analysis results for complexes **1** – **3** are consistent with the presence of two nickel centers for each complex.

Table 1 Electronic spectra and electrochemical data for complexes **1** – **3**, at 25ºC.

Complex	**λ_{max}, nm (ε, L mol^{-1} cm^{-1})**	**E_{pc}, (V *vs* NHE)**	**E_{pa}, (V *vs* NHE)[a]**
	CH_3CN	CH_3CN	
A	604 (20)	-1.27 and -1.64	
1	609 (14)	-0.960	-0.974
2	616 (15)	-0.850	
3	626 (23)	-0.943	-0.916
B	621 (20)	-1.29 and -1.66	1.00 and 1.40

[a][Complexes] = 1 × 10^{-3} mol L^{-1}; **B** = $[Ni^{II}Ni^{II}(L)(\mu\text{-}CH_3COO)_2(OH_2)]BPh_4 \cdot H_2O$ L= 2-[(4,7-diisopropyl-1,4,7-triazonan-1-yl)methyl]-4-methyl-6[(pyridine-2-ylmethylamino)methyl]phenolate [27]. Conditions for electrochemistry: glassy carbon (working); platinum wire (counter); and Ag/Ag^+ (reference). Ferrocene (E° = 0.4 V *vs* NHE) was used as the internal standard.

3.4 *Potentiometric equilibrium studies*

Potentiometric titrations of complexes **1** – **3** were carried out in CH_3CN/H_2O (1:1) solutions in order to assess the presence of water molecules coordinated to the Ni(II) metal centers, since the lability of the acetate bridges is facilitated by increasing the pH of the solution [7,11,23,101,102,103], which generates aquo-complexes. The results indicate the neutralization of 7 mols of potassium hydroxide per mol of complex in the pH range of 3.00 – 12.00. The corresponding pK_a values are listed in Table 2 and the proposed assignments of the corresponding equilibrium observed for complexes **1** – **3** are shown in Figure 2. The species distribution curves as a function of pH for complexes **1** – **3** are presented in Figure 3.

For complexes **1** – **3**, the first pK_a can be assigned to the release and the deprotonation of one acetate bridge bonded to the metal centers, leading to the $[(H_2O)_2Ni^{II}(\mu\text{-OAc})Ni^{II}(OH_2)]$ species. The second pK_a can be assigned to the release and the deprotonation of the second acetate bridge, leading to the $[(H_2O)_3Ni^{II}Ni^{II}(OH_2)]$ species.

Table 2. Values of the protonation constants for complexes **1** – **3**.

	1	**2**	**3**	
pK_{a1}	5.09±0.02	5.07±0.17	5.27±0.15	Acetate
pK_{a2}	5.62±0.04	5.83±0.11	5.69±0.03	acetate
pK_{a3}	5.92±0.09	6.99±0.13	6.80±0.19	water
pK_{a4}	6.35±0.17	7.31±0.09	7.99±0.06	water
pK_{a5}	7.67±0.30	9.08±0.24	8.64±0.14	water
pK_{a6}	9.38±0.16	10.65±0.09	10.24±0.15	amine
pK_{a7}	10.93±0.11	11.51±0.21	11.01±0.17	amine

The deprotonation of a metal-bound water molecule leads to the μ-OH bridge, yielding the species $[(OH_2)_2Ni^{II}(\mu\text{-OH})Ni^{II}(OH_2)]$. The p$K_{a4}$ and pK_{a5} can be attributed to the deprotonation of water molecules bonded to the metal centers and can be tentatively attributed to the species $[(OH_2)(OH)Ni^{II}(\mu\text{-OH})Ni^{II}(OH_2)] \rightleftharpoons [(OH_2)(OH)Ni^{II}(\mu\text{-OH})Ni^{II}(OH)]$. These attributions are in

agreement with those for previous Ni(II) complexes described in the literature [11,27,42,43,104] and the lower values obtained for pK_{a4} and pK_{a5} may be interpreted in terms of electrostatic interactions between the protonated amino groups in the side chain of the complexes and the water molecules bound to the metal centers [51,61]. The last two deprotonation constants (pK_{a6} and pK_{a7}) can be assigned to the protonation/deprotonation of the amines in the side chain of complexes **1** – **3**, which is in agreement with the values for free amines in solution [105].

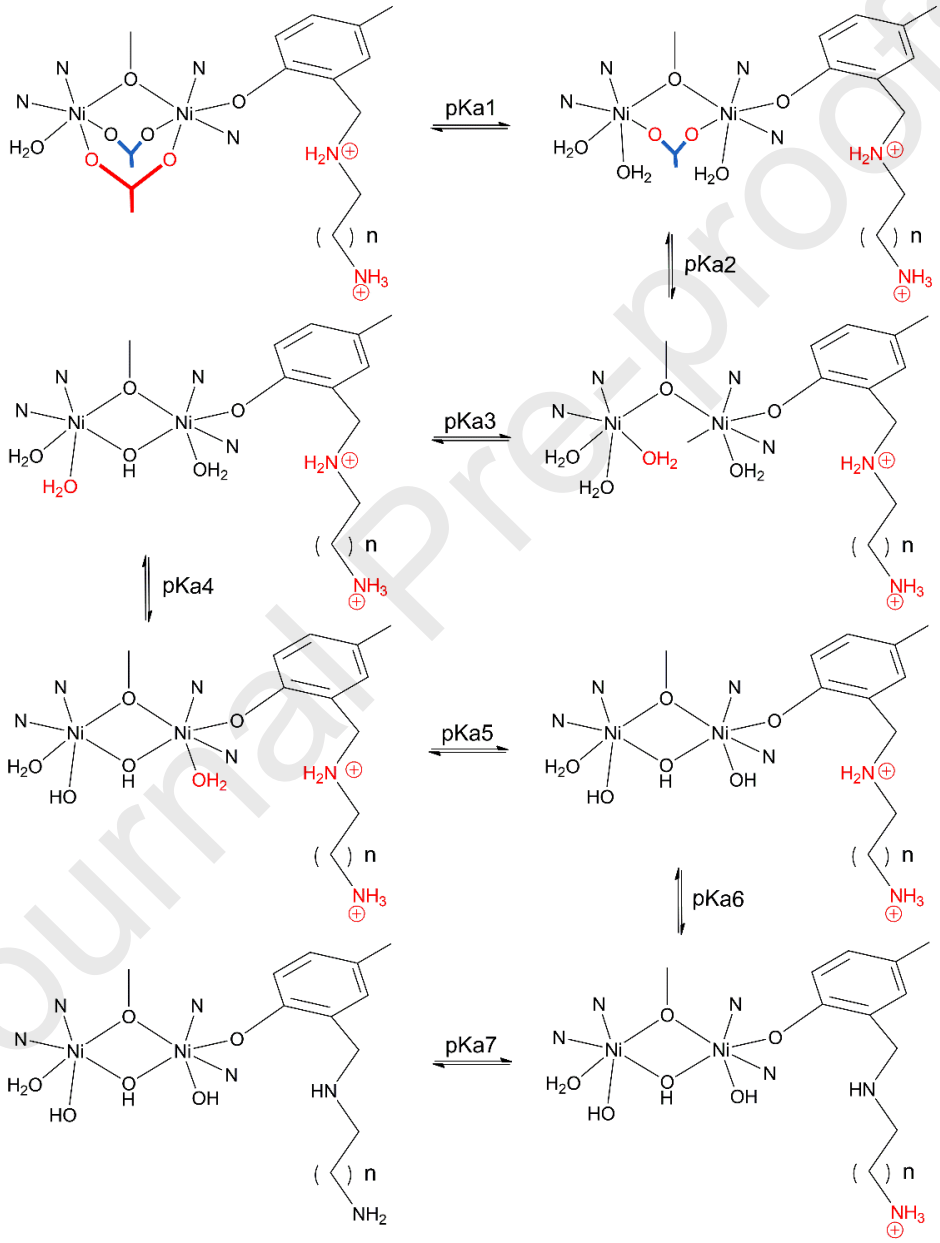

Figure 2. Proposed assignment of observed protonation equilibria for complexes **1** – **3** in CH_3CN/H_2O 1:1 v/v solution; I = 0.1 mol L^{-1} (KCl) at 25 ºC.

3.5 *Reactivity studies*

Kinetics experiments were carried out in order to determine the influence of hydrogen bonding on the hydrolysis of phosphoesters using the activated substrate 2,4-BDNPP under pseudo-first-order conditions ([S]>> [complex]). The hydrolysis activities were investigated in an CH_3CN/H_2O (1:1 v/v) mixture in the pH range 5.00 – 9.50 for complexes **1** and **3** and 5.00 – 9.00 for complex **2**. The reaction was monitored spectrophotometrically at 400 nm, corresponding to the maximum absorption of the product 2,4-dinitrophenolate (2,4-DNP). The pH dependence of the catalytic activity for the three complexes was obtained from the plot of k_{obs} *versus* pH (Figure 3). It was not possible to determine the kinetic pK_a values for any of the three complexes but, as can be seen in Figure 3, for all complexes the k_{obs} is highly influenced by alkaline pH.

Comparing to the complex **A**[43], that presented an exponential dependence on the pH, it is possible to observe a change in the k_{obs} *vs* pH dependence profile for complexes **1** – **3** (dots in Figure 3). The profile of k_{obs} for complexes **1** – **3**, with amino groups in the side chain, presents a bell-type shape at pH values ranging from 5.00 to 8.50 for complexes **1** and **2**, and 5.00 to 7.50 for complex **3**, and then a leap at pH 9.00. The non-negligible catalytic activity presented by complexes **1** – **3** (Tables S5 – S7) in low-pH regions – when compared to other Ni(II) complexes reported in the literature [17,39,42,43,47] – can probably be explained by interactions involving the protonated amino groups in the side chain of the complexes and a water molecule coordinated to the metal center. These interactions may lead to the lowering of the pK_a of the metal-bound water molecule, which generates the required species for the hydrolysis reaction to occur, i.e., with a hydroxo molecule coordinated to the metal center.

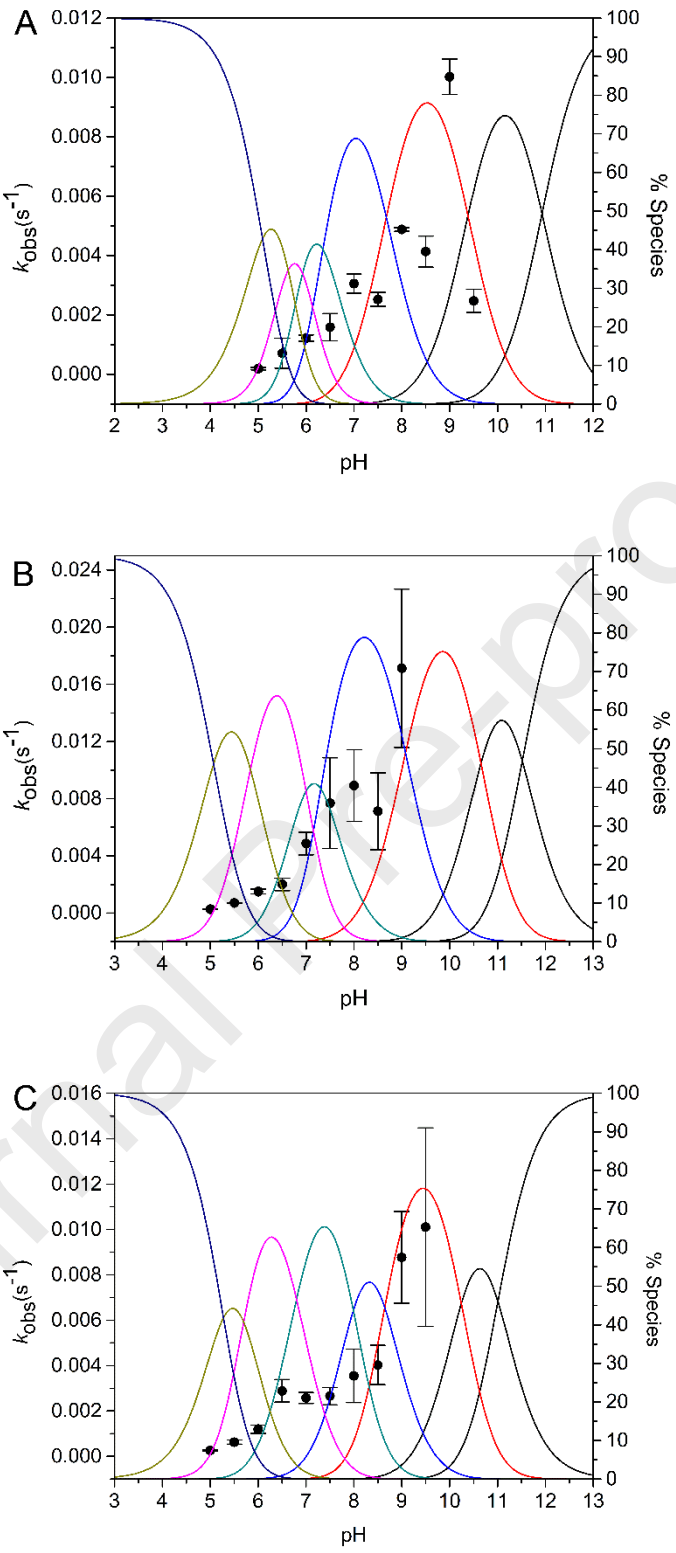

Figure 3. The k_{obs} *vs* pH plot for the hydrolysis reaction of the 2,4-BDNPP (represented as black circles) promoted by complexes **1** (A), **2** (B) and **3** (C) in CH_3CN/H_2O (50% v/v) at 25º C. [Complex] = 1.00×10^{-5} to 4.00×10^{-6} mol L^{-1}; [2,4-BDNPP] = 1.07×10^{-3} to 3.73×10^{-3} mol L^{-1}, along with the species distributions shown as solid lines.

The dependence of the reaction rate on the substrate concentration was investigated at each pH value, in the pH range of 5.00 – 9.50 for complexes **1** and **3** and 5.00 – 9.00 for complex **2**. In these experiments it was observed that, for all complexes and pH values, initially, the hydrolysis rate increases linearly at low substrate concentrations and reaches saturation as the concentration increases, which suggests the formation of a complex–substrate intermediate (Figure 4). The Michaelis-Menten [106] model was employed to obtain the kinetic parameters. The kinetic data for complexes **1** – **3** and similar compounds described in the literature, with and without second coordination sphere, are listed in Table 3.

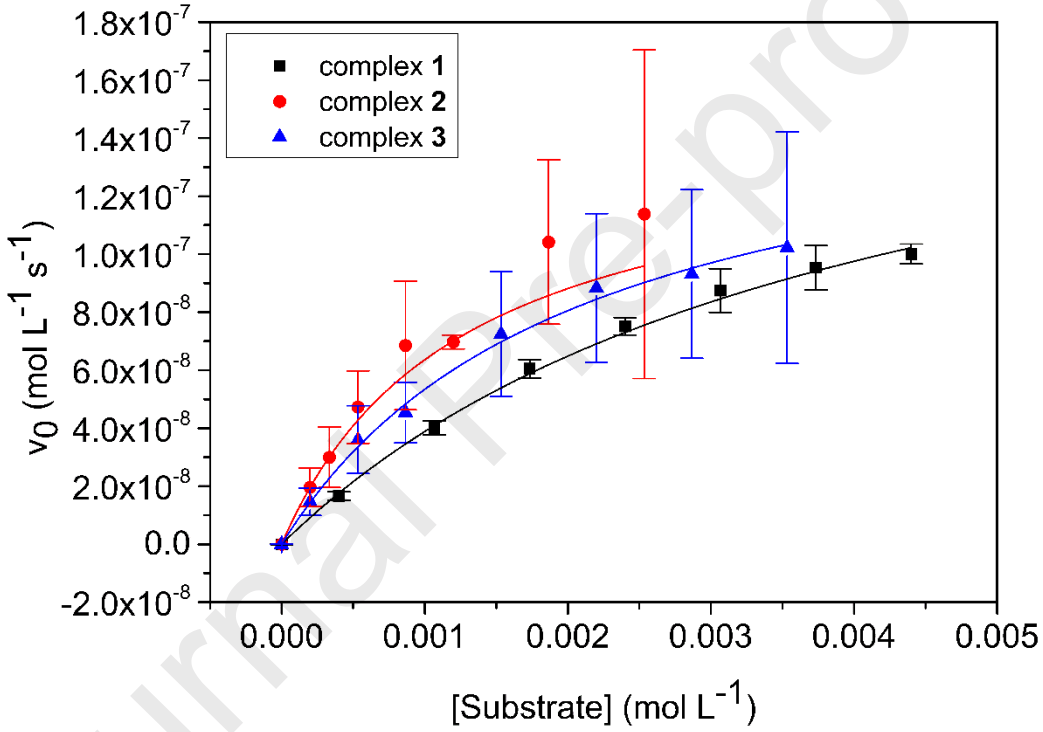

Figure 4. Dependence of the initial reaction rate (v_0) on the 2,4-BDNPP concentration for the hydrolysis reaction promoted by complexes **1** - **3**. Conditions: [complex] = 4.00×10^{-6} mol L^{-1} for complexes **1** and **2**; [complex] = 5.18×10^{-6} for complex **3**; [buffer] = 50.00×10^{-3} mol L^{-1} (CHES, pH = 9.00); $I = 50.00 \times 10^{-3}$ mol L^{-1} ($LiClO_4$) in CH_3CN/H_2O (50% v/v) at 25 ºC.

Table 3 Kinetic parameters of complexes **1** – **3** for 2,4-BDNPP hydrolysis and other complexes for comparison.

Complex	$v_{max} \times 10^7$ (mol L^{-1} s^{-1})	$K_M \times 10^3$ (mol L^{-1})	$k_{cat} \times 10^2$ (s^{-1})	K_{ass} (L mol^{-1})	k_{cat}/K_M (L s^{-1} mol^{-1})	$f \times 10^{-4}$ [a]	pH
A [b]	5.37	1.57	5.37	637.0	34.20	13.84	9.00
1	1.97±0.11	4.06±0.35	4.92±0.27	246.3	12.11±1.24	12.67	9.00
1	0.30±0.01	2.03±0.16	0.30±0.01	492.6	1.47±0.12	1.55	6.50
2	1.40±0.18	1.20±0.31	3.50±0.45	833.3	29.18±8.35	9.02	9.00
2	0.31±0.009	1.30±0.07	0.31±0.01	769.2	2.38±0.15	1.60	6.50
3	1.64±0.12	2.07±0.23	3.16±0.23	483.1	15.30±2.03	8.15	9.00
3	0.64±0.03	1.38±0.12	0.37±0.02	724.6	2.69±0.27	1.92	6.50
B [c]	1.33	3.44	1.26	291	3.70	3.25	9.00
C [d]	0.58	1.19	3.42	840.3	28.82	8.84	9.00
D [e]		0.21	0.28	4762	0.01		7.00
E [f]	0.34	27.8	0.07	36.0	0.02	2.11	6.50
F [g]		3.07	0.194	325	0.63	1.00	6.50

[a] $f = k_{cat}/k_{unc}$ (catalytic factor), where $k_{unc} = 3.88 \times 10^{-7}$ s^{-1} at 25 ºC and pH = 9.00; $k_{unc} = 1.93 \times 10^{-7}$ s^{-1} at 25 ºC and pH = 6.50 [78]; [b] $[Ni_2(HBPPAMFF)(\mu OAc)_2(H_2O)]BPh_4$, H_2BPPAMFF = 2-[(***N***-benzyl-***N***-2-pyridylmethylamine)]-4-methyl-6-[*N*-(2-pyridylmethyl)aminomethyl)]-4-methyl-6-formylphenol [43]; [c] $[Ni^{II}Ni^{II}(L)(\mu\text{-}CH_3COO)_2(OH_2)]BPh_4 \cdot H_2O$, L = 2-[(4,7-diisopropyl-1,4,7-triazonan-1-yl)methyl]-4-methyl-6[(pyridine-2-ylmethylamino)methyl]phenolate [27]; [d] $[Ni_2(L1)(OAc)_2(H_2O)]ClO_4 \cdot H_2O$, L1 = 2-[*N*-bis(2-pyridylmethyl)aminomethyl]-4-methyl-6-[*N*-(2-pyridylmethyl)aminomethyl]]phenol [42]; [e] $[Ni_2(L^{Cl}O)(\mu\text{-}OAc)_2](PF_6) \cdot 3H_2O$, L = 2,6-bis[bis(2-pyridylmethyl)aminomethyl]-4-clorophenol [107]; [f] $[FeZn(IPCPMP)(OAc)_2(CH_3OH)]PF_6$, IPCPMP = 2-(*N*-isopropyl-*N*-((2-pyridyl)methyl)aminomethyl)-6-(*N*-(carboxylmethyl)-*N*-((2-pyridyl)methyl)aminomethyl)-4-methylphenol [108]; [g] $[FeZn(L_1bpea\text{-}apur)(\mu\text{-}OH)(H_2O)]ClO_4$, L_1bpea-apur = 2-((2-(9*H*-Purin-6-ylamino)ethylamino)methyl)-6-(((3-((bis(2-(pyridin-2-yl)ethyl)amino)methyl)-2-hydroxy-5-methylbenzyl)(pyridin-2-ylmethyl)amino)methyl)-4-methyl-phenol [76].

The derivatization with pendant amino groups in the complexes **1** and **3** led the K_M values higher when compared to those obtained for complex **A** [43] (with the aldehyde ligand H_2BPPAMFF), **C** [42] (with a dinucleating ligand with three pyridines metal-donor groups attached) and **D** [107] (with a very similar ligand reported in this study and presenting four pyridines units). Thus, there is a decrease in the K_{ass}, together with a decrease in k_{cat} leading to an overall catalytic efficiency lower than that of complexes **A** [43] and **C** [42]. A similar behavior was presented by complex **B**, reported by Xavier *et al*, which presented a triazacyclononane macrocyclic ring unit in its structure (Table 3). Also, the hydrolysis reaction with complex **1** was 126,700 times faster than the uncatalyzed reaction ($k_{unc} = 3.88 \times 10^{-7}$ s^{-1} at 25 ºC) [78], which is comparable to the value found for complex **A** [43], despite the lower catalytic efficiency value presented for **1**. This can

be explained by the fact that complex **1** presented the highest k_{cat} value among the three complexes. The hydrolysis reaction with complex **2** was 90,200 times faster than the uncatalyzed reaction (k_{unc} = 3.88 × 10^{-7} s^{-1} at 25 ºC) [78] and showed a decrease in both K_M and k_{cat} when compared to complex **A** [43], presenting the highest K_{ass} value of the three complexes with amino groups, as well as the highest catalytic efficiency. Figure 5 illustrates the behavior of f (k_{cat}/k_{unc}) for the substrate 2,4-BDNPP hydrolysis with respect to pH for the three complexes.

As can be seen from the Table 3, complexes **1** – **3** presents higher catalytic efficiency if compared with analogous $Fe^{III}Zn^{II}$ complexes in the same pH values. Complex **F** [76], reported by Pereira *et al*, with an aminopurine group as side chain moiety of the ligand, present a meaningful second coordination sphere effect regarding the hydrolysis of the 2,4-BDNPP substrate, while complex **E** [108], reported by Jarenmark *et al* has no such effect. From the values listed in Table 3, it is possible to observe a notable increase not only in the catalytic efficiency of the systems containing Ni(II), but also in the k_{cat} and in the catalytic acceleration factor *f*. The catalyzed hydrolysis reaction for the complexes **1** – **3** was 1.50, 1.60 and 1.92 (for **1**, **2** and **3** respectively) times faster than the hydrolysis reaction promoted by complex **F** [76] at pH 6.50, indicating that even at lower pH values (Table S5 – S7), the complexes studied in this work are more active than other analogues complexes reported in the literature and presenting phosphoesterase activity [61,76,108].

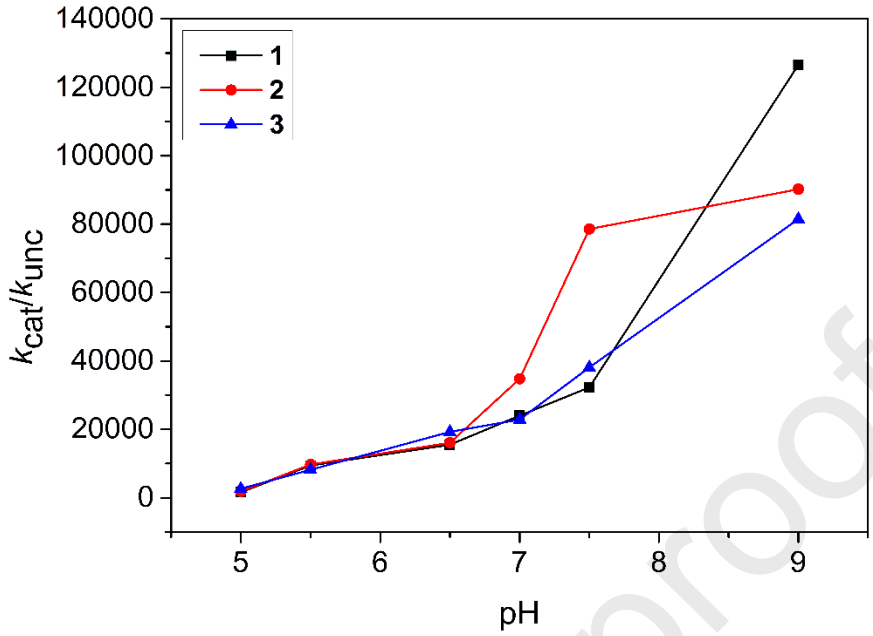

Figure 5 Plot of f (k_{cat}/k_{unc}) *vs* pH for the three complexes, using the substrate 2,4-BDNPP. pH 5.00, k_{unc} = 1.77 × 10^{-7} s^{-1}; pH 5.5, k_{unc} = 1.22 × 10^{-7} s^{-1}; pH 6.50, k_{unc} = 1.93 × 10^{-7} s^{-1}; pH 7.00, k_{unc} = 1.89 × 10^{-7} s^{-1}; pH 7.50, k_{unc} = 1.82 × 10^{-7} s^{-1}; pH 9.00, k_{unc} = 3.88 × 10^{-7} s^{-1} [78].

To improve our understanding of the catalytic process, the phosphate conjugates of complexes **1 – 3** were optimized and are shown in Figure 6. As can be seen, one minimum-energy structure for all phosphate conjugates was found after a proton transfer between the charged amine and a hydroxy group coordinated to the nickel center, in which complex **2** also shows a relevant interaction between the amine and an oxygen atom present in the substrate. This additional interaction with the substrate may explain the higher catalytic efficiency obtained with it.

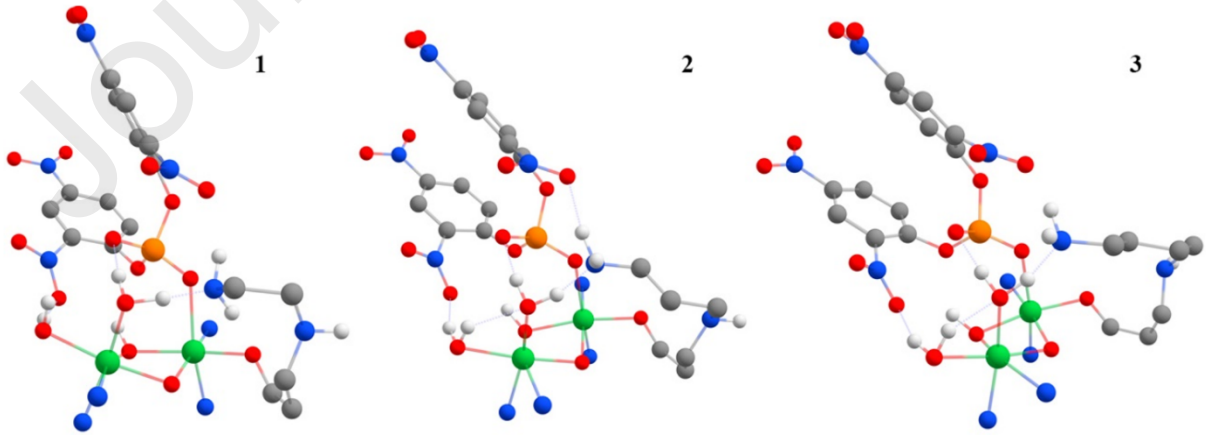

Figure 6. Optimized ground state geometries for the phosphate conjugates of **1**, **2** and **3** using BP86/DEF2-TZVP (metals) or DEF2-SVP (all others). Some atoms are omitted for clarity.

In order to assess the possible hydrolysis of the monoester 2,4-DNPP, a stoichiometric reaction between complexes **1** – **3** and the 2,4-BDNPP substrate was monitored. It was observed that 2 equivalents of 2,4-DNP are released over a period of 40 h, at 25 °C, which indicates the hydrolysis of both the mono- and the diester. Based on this information, and assuming that the hydrolysis of 2,4-BDNPP leads to the formation of an intermediate (presumably the monoester coordinated to the catalyst), the catalytic activity of the most efficient complex **2** towards the hydrolysis of the monoester 2,4-DNPP was also investigated. The determination of the initial rates as a function of the substrate concentration reveals saturation kinetics presenting Michaelis-Menten behavior (Figure 7). It was possible to obtain values of k_{cat} = 9.60 × 10^{-3} s^{-1} and K_{ass} = 3833.34 mol L^{-1}, revealing that the constant for the association of the monoester with catalyst **2** is 4 times larger, while the k_{cat} is 3.6 times lower when compared to the parameters obtained with the corresponding 2,4-BDNPP diester. Also, complex **2** hydrolyzes 2,4-DNPP 35,400 times faster (f = 3.54 × 10^{4} s^{-1}) than the uncatalyzed reaction (k_{unc} = 2.71 × 10^{-7} s^{-1} at 25 ºC) [109]. As the 2,4-DNPP substrate is a dianion, it could have coordinated with the complex in bridging mode so that the μ-OH could act as the nucleophile, which may explain the lower k_{cat} value presented by **2** in the hydrolysis reaction of 2,4-DNPP.

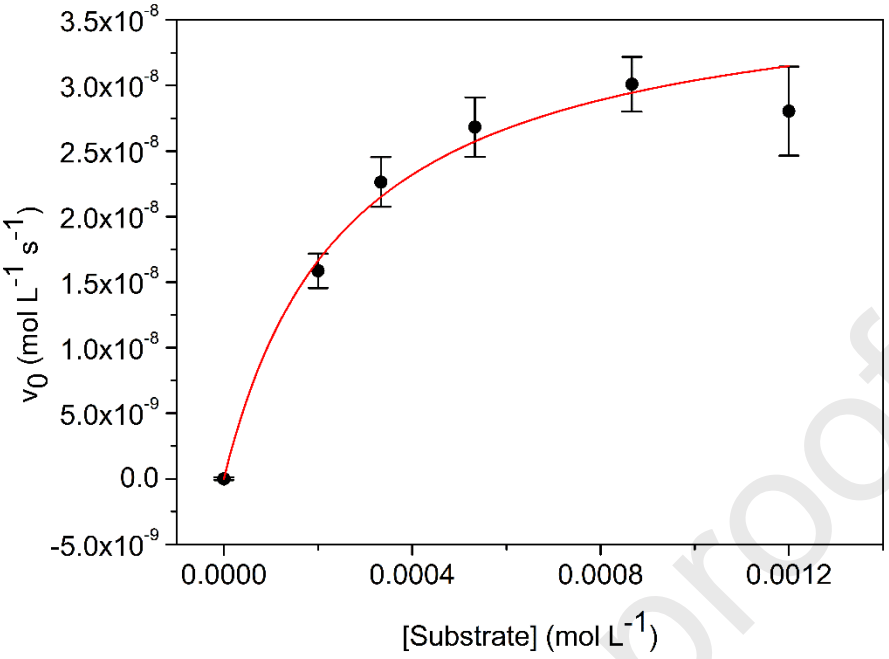

Figure 7. Dependence of the initial reaction rate (v_0) on the monoester 2,4-DNPP concentration for the hydrolysis reaction promoted by complex **2**. Conditions: [complex] = 4.00×10^{-6} mol L^{-1}; [buffer] = 50.00×10^{-3} mol L^{-1} (CHES, pH = 9.00); I = 50.00×10^{-3} mol L^{-1} ($LiClO_4$) in CH_3CN/H_2O (50% v/v) at 25 ºC.

In order to obtain the number of catalytic cycles for the hydrolysis of the 2,4-BDNPP, a hydrolysis reaction promoted by complexes **1** – **3** (4×10^{-6} mol L^{-1}) and the 2,4-BDNPP substrate (2×10^{-4} mol L^{-1}) was monitored at 445 nm, at pH 9.00 and 25 °C, revealing that the complexes can be considered as efficient catalysts and are able to hydrolyze 42 molecules of substrate in 24 h for complex **1**, 58 molecules in 12 h for complex **2** and 41 molecules in 8 h for complex **3**.

To establish whether a general base catalysis or an intramolecular nucleophilic attack can be attributed to complexes **1** – **3**, the isotopic effect was evaluated in the hydrolysis of 2,4-BDNPP, under identical conditions using either H_2O or D_2O. The values for k_H/k_D for complexes **1**, **2** and **3** were, respectively, 5.22, 4.22 and 7.02, indicating that there is a proton transfer in the rate-limiting step of the reaction ($k_H/k_D>2$) [110], suggesting a general base reaction mechanism.

The effect of the temperature on the hydrolysis reaction was investigated under the same conditions described above for the substrate excess experiments at 20, 25, 30, 35 and 40 ºC. The activation parameters E_a, $\Delta H^{\neq}$, $T\Delta S^{\neq}$ and $\Delta G^{\neq}$ for the hydrolysis catalyzed by complexes **1** – **3**

were obtained through the Arrhenius and the Eyring equations [111] and the results are reported in Table 4.

Table 4. Activation parameters for the hydrolysis of 2,4-BDNPP.

Complex	E_a (kJ mol^{-1})	$\Delta H^{\neq}$ (kJ mol^{-1})	$T\Delta S^{\neq}$ (kJ mol^{-1})[a]	$\Delta G^{\neq}$ (kJ mol^{-1})
1	39.44	36.93	-47.07	84.00
2	68.86	66.34	-17.23	83.57
3	106.17	103.66	17.43	86.23
HO^{-}[b]		80	-107	111

[a]At 298.15 K, [b]General basic catalysis [112]

As observed, the data indicates that for complexes **1** and **2** an organization of the reactive species occurs in the TS ($\Delta S^{\neq} < 0$), while for complex **3** a value of $\Delta S^{\neq} > 0$ suggests that the reactive species becomes less structured in the TS. For all complexes $\Delta H^{\neq} > 0$, which reflects bond breaking in the activated complex. For the calculated phosphate conjugates, there was an increase in the distance of the hydrogen bond connecting the lateral amine and the coordinated water from 1.475 Å for **1** to 1.617 Å for **3**, and as obtained from the Eyring plots, the enthalpic contribution to the activation barrier also increases from **1** to **3**. Both results suggest a mechanism where the water transfers one proton back to the amine before the phosphate hydrolysis. The higher entropic effect caused by the elongation of the carbon chain, that hence loses more degrees of freedom with binding, can also be observed from **1** to **3**, in agreement with the change in entropy from -47.07 kJ mol^{-1} for **1** to 17.43 kJ mol^{-1} for **3**.

3.5.1 Proposed reaction mechanism for 2,4-BDNPP hydrolysis by complexes **1** – **3**

Based on the data detailed above, the reaction mechanism shown in Scheme 2 is proposed for the hydrolysis of the 2,4-BDNPP substrate by complexes **1** – **3**. First, the protonated amine transfers a proton to the hydroxo molecule bound to the Ni^{II} center on the hard side of the complex, which generates the [$(H_2O)(OH)Ni^{II}(\mu$-$OH)Ni^{II}(H_2O)$] unit. The substrate then binds in a monodentate fashion to the Ni(II) ion by displacing its labile H_2O ligand. For complexes **1** and **3** a mechanism

is suggested in which the Ni^{II}-bound hydroxide activates an H-bonded water molecule to act as the reaction-initiating nucleophile [76,113] (Figure 9), with concomitant release of the 2,4-DNP leaving group. Since stoichiometric reactions between complexes **1** – **3** and 2,4-BDNPP released 2 equiv. of 2,4-DNP, it is proposed that after the release of the first 2,4-DNP unit an intramolecular nucleophilic attack of the μ-OH would be responsible for the hydrolysis of the bound monoester. The remaining phosphate is then displaced by excess water, regenerating the catalytic center. For complex **2** a very similar mechanism is proposed, in which the sole difference is the interaction between the amine group and the substrate, which increases the proximity of the substrate and the complex, explaining its higher catalytic efficiency when compared to complexes **1** and **3**.

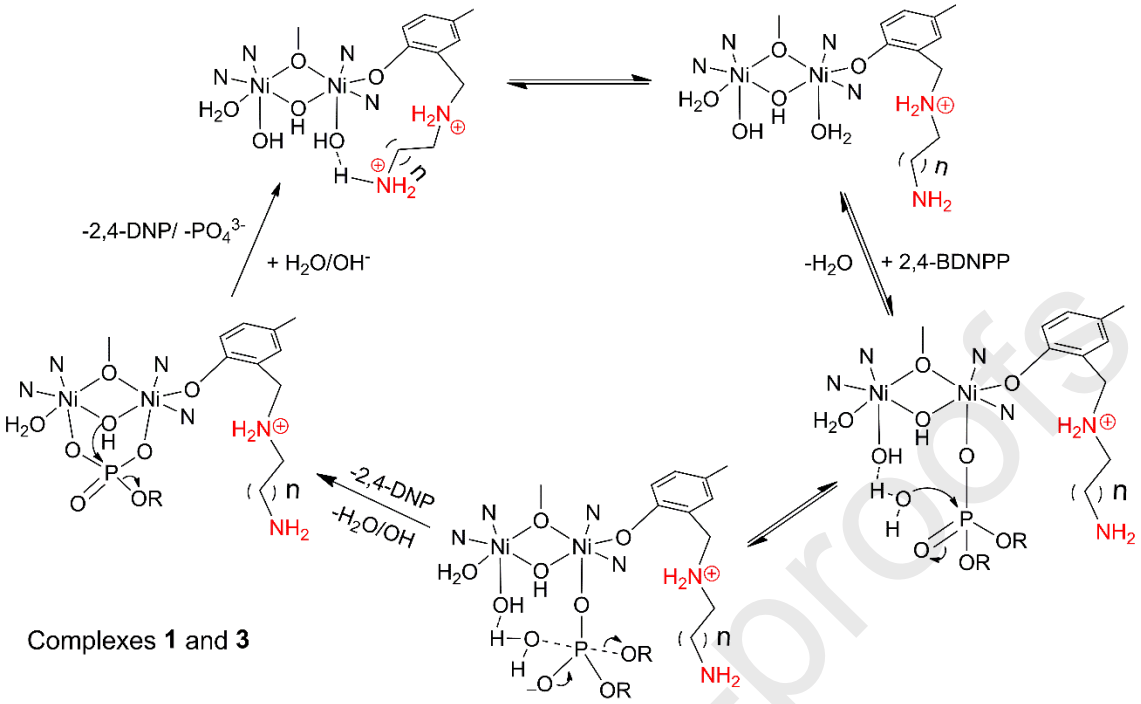

Complexes **1** and **3**

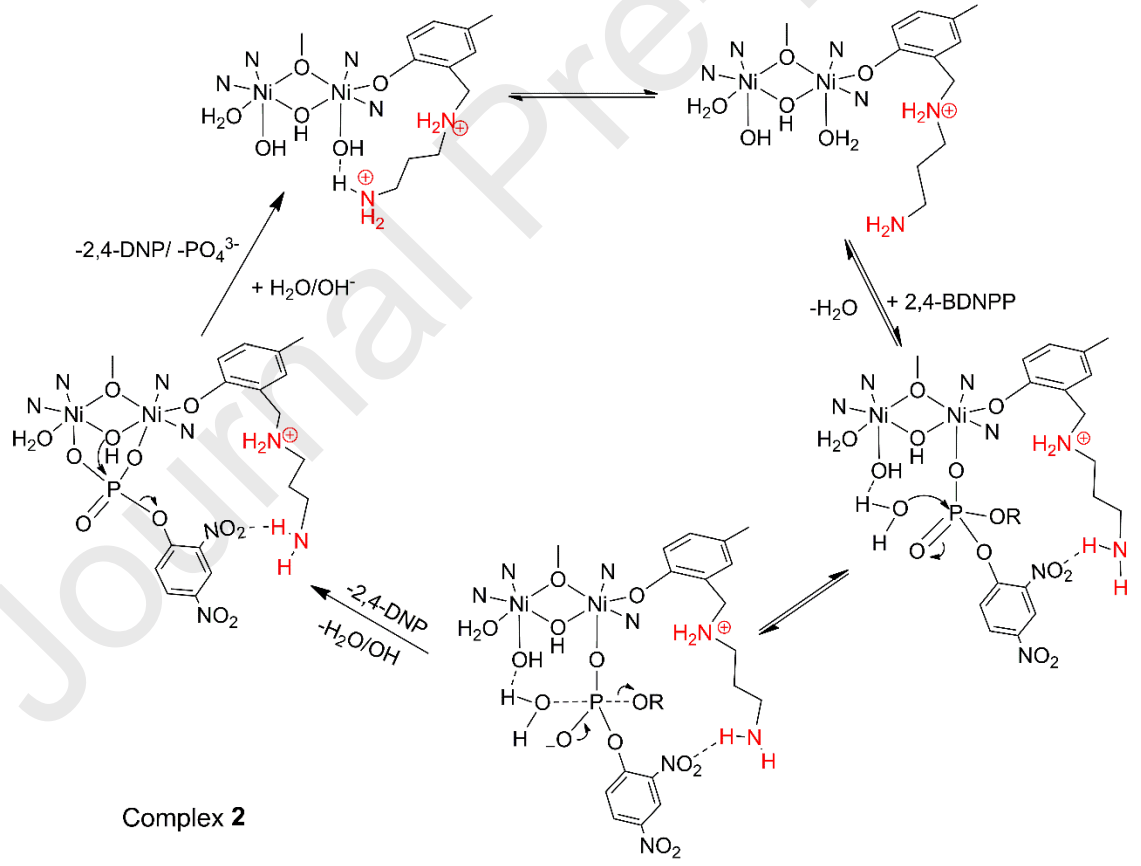

Complex **2**

Scheme 2. Proposed mechanism for hydrolysis of 2,4-BDNPP substrate promoted by complexes **1** and **3** (top) and **2** (bottom).

4. **Antibacterial activity**

The three Ni(II) complexes were tested for their antibacterial activity against three Gram-negative (*Salmonella enterica*, *Pseudomonas aeruginosa* and *Escherichia coli*) and three Gram-positive (*Staphylococcus aureus*, *Aeromonas hydrophila* and *Listeria innocua*) bacteria. Table 5 shows the values obtained for the minimum inhibitory concentration and the minimum bactericidal concentration for complexes **1** – **3**. As can be seen, complex **2** showed significant *in vitro* antibacterial activity against all Gram-positive and Gram-negative bacteria used in this study. Notably, the inhibitory (7.81 μg mL^{-1}) and antibacterial (31.25 μg mL^{-1}) activity against *S. aureus* was observed at relatively low concentrations. The other two complexes also presented inhibitory and bactericidal activity against *S. aureus*, although at higher concentrations compared with complex **2**, but still in good agreement with values reported in the literature [73-75,114-117].

Table 5. Antimicrobial activity of metal complexes evaluated by MIC and MBC (µg/mL), pH=7.2.

Complex	***Salmonella Typhimurium* ATCC 14028**		***Pseudomonas aeruginosa* ATCC 27853**		***Escherichia coli* ATCC 25922**		***Staphylococcus aureus* *ATCC* 25923**		***Aeromonas hydrophila* ATCC 7966**		***Listeria innocua* ATCC 33090**	
	MIC µg/mL	**MBC µg /mL**	**MIC µg/mL**	**MBC µg /mL**	**MIC µg/mL**	**MBC µg /mL**	**MIC µg/mL**	**MBC µg /mL**	**MIC µg/mL**	**MBC µg /mL**	**MIC µg/mL**	**MBC µg /mL**
1	>1000	>1000	>1000	>1000	>1000	>1000	31.25	125	>1000	>1000	>1000	>1000
2	62.5	62.5	125	250	62.5	62.5	7.81	31.25	62.5	250	62.5	250
3	>1000	>1000	>1000	>1000	>1000	>1000	7.81	31.25	>1000	>1000	>1000	>1000

5 **Conclusions**

We synthesized and characterized three new unsymmetric ligands derived from H_2BPPAMFF, and also synthesized their respective Ni(II) complexes. The phosphoesterase activity (using the model substrates 2,4-BDNPP and 2,4-DNPP) of **1** – **3** was found to be lower than that presented by complex **1b**, and the derivatizations led to a decrease in the k_{cat} values for complexes **1** – **3** when compared with complex **1b**. On the other hand, the insertion of the amino groups in the side chain of the ligands led to a lowering of the pH values at which the complexes are able to catalyze the hydrolysis of the 2,4-BDNPP substrate. Thus, complexes **1** – **3** presented catalytic activity at pH values close to physiological pH, which can be attributed to interactions between the amino groups and water molecules bound to the metal center. In tests to determine the antibacterial activity, complexes **1** – **3** also showed inhibitory and bactericidal action (based on MIC and MBC results), and complex **2** showed the best results against Gram-positive and Gram-negative bacterial strains.

Acknowledgments

This study was financed in part by the Coordenação de Aperfeiçoamento de Pessoal de Nível Superior - Brasil (CAPES) - Finance Code 001. The authors are grateful to CNPq, INCT-Catálise, CAPES – PrInt Project number 88887.310569/2018-00 and FAPESC for financial support.

6 **References**

1. Wilcox, D. E. Chem. Rev., 96, (1996) 2435-2458, https://doi.org/10.1021/cr950043b
2. Lehninger, A. L., Nelson, D. L., Cox, M. M., & Cox, M. M., Lehninger principles of biochemistry, Macmillan, 2005.
3. Das, B., Daver, H., Pyrkosz-Bulska, M., Persch, E., Barman, S. K., Mukherjee, R., Gumienna-Kontecka, E., Jarenmark, M., Himo, M., Nordlander, E., J. Inorg. Biochem., 132, (2014) 6-17, https://doi.org/10.1016/j.jinorgbio.2013.08.001
4. Erxleben, A. Front. Chem., *7*, (2019) 82. https://doi.org/10.3389/fchem.2019.00082
5. Desbouis, D., Troitsky, I. P., Belousoff, M. J., Spiccia, L., Graham, B., Coord. Chem. Rev., 256, (2012) 897-937, https://doi.org/10.1016/j.ccr.2011.12.005
6. Dupureur, C., Curr. Op. Chem. Bio., 12, (2008) 250-255, https://doi.org/10.1016/j.cbpa.2008.01.012

7. Gahan, L. R., Smith, S. J., Neves, A., Schenk, G., Eur. J. Inorg. Chem., (2009) 2745-2758, https://doi.org/10.1002/ejic.200900231
8. Yamaguchi, K., Akagi, F., Fujinami, S., Suzuki, M., Shionoya, M., Suzuki, S., Chem. Commun., (2001) 375-376, https://doi.org/ 10.1039/b008994j
9. Daumann, L. J., Schenk, G., Ollis, D. L., Gahan, L. R., Dalton Trans., 43, (2014) 910-928, https://doi.org/10.1039/c3dt52287c
10. Camargo, T. P., Maia, F. F., Chaves, C., Souza, B., Bortoluzzi, A. J., Castilho, N., Bortolotto, T., Terenzi, H., Castellano, E. E., Haase, W., Tomkowicz, Z., Peralta, R. A., Neves, A., J. Inorg. Biochem., 146, (2015) 77-88, https://doi.org/10.1016/j.jinorgbio.2015.02.017
11. Mitić, N., Smith, S. J., Neves, A., Guddat, L. W., Gahan, L. R., Schenk, G., Chem. Rev., 106, (2006) 3338-3368, https://doi.org/10.1021/cr050318f
12. Schenk, G., Mitić, N., Hanson, G. R., Comba, P., Coord. Chem. Rev., 257, (2013) 473-482, https://doi.org/10.1016/j.ccr.2012.03.020
13. Cowan, J. A., Curr. Op. Chem. Bio., 5, (2001) 634-642, https://doi.org/10.1016/S1367-5931(01)00259-9
14. Shell, T. A., Mohler, D. L., Curr. Org. Chem., 11, (2007) 1525-1542, https://doi.org/10.2174/138527207782418654
15. Buchholz, R. R., Etienne, M. E., Dorgelo, A., Mirams, R. E., Smith, S. J., Chow, S. Y., Hanton, L. R., Jameson, G. B., Schenk, G., Gahan, L. R., Dalton Trans., 43, (2008) 6045-6054, https://doi.org/10.1039/b806391e
16. Livieri, M., Mancin, F., Saielli, G., Chin, J., Tonellato, U., Chem. Eur. J., 13, (2007) 2246-2256, https://doi.org/10.1002/chem.200600672
17. Bhardwaj, V. K., Singh, A., Inorg. Chem., 53, (2014) 10731-10742, https://doi.org/10.1021/ic501961d
18. Suh, J., Acc. Chem. Res., 25, (1992) 273-279, https://doi.org/10.1021/ar00019a001
19. Hegg, E. L., Burstyn, J. N., Coord. Chem. Rev., 173, (1998) 133-165, https://doi.org/10.1016/S0010-8545(98)00157-X
20. Schenk, G., Mitić, N., Gahan, L. R., Ollis, D. L., McGeary, R. P., Guddat, L. W., Acc. Chem. Res., 45, (2012) 1593-1603, https://doi.org/10.1021/ar300067g

21. Yu, Z., Cowan, J. A., Curr. Op. Chem. Bio., 43, (2018) 37-42, https://doi.org/10.1016/j.cbpa.2017.10.029
22. Barone, G., Terenzi, A., Lauria, A., Almerico, A. M., Leal, J. M., Busto, N., García. B., Coord. Chem. Rev., 257, (2013) 2848-2862, https://doi.org/10.1016/j.ccr.2013.02.023
23. Lanznaster, M., Neves, A., Bortoluzzi, A. J., Aires, V. V. E., Szpoganicz, B., Terenzi, H., Severino, P. C., Fuller, J. M., Drew, S. C., Gahan, L. R., Hanson, G. R., Riley, M. J., Schenk, G., J. Biol. Inorg. Chem., 10, (2005) 319-332, https://doi.org/10.1007/s00775-005-0635-7
24. Pages, B. J., Ang, D. L., Wright, E. P., Aldrich-Wright, J. R., Dalton Trans., 44, (2015) 3505-3526, https://doi.org/10.1039/c4dt02700k
25. Maranha, F. G., Silva, G. A. S., Bortoluzzi, A. J., Nordlander, E., Peralta, R. A., Neves, A., Inorganica Chim. Acta, (2019) 119280, https://doi.org/10.1016/j.ica.2019.119280
26. Jarenmark, M., Csapó, E., Singh, J., Wöckel, S., Farkas, E., Meyer, F., Haukka, M., Noedlander, E., Dalton Trans., 39, (2010) 8183-8194, https://doi.org/10.1039/b925563j
27. Xavier, F. R., Neves, A., Polyhedron, 109, (2016) 59-66, https://doi.org/10.1016/j.poly.2016.02.013
28. Heying, R.S., Silva, M. P., Wecker, G. S., Peralta, R. A., Bortoluzzi, A. J., Neves, A., Inorg. Chem. Commun., 102, (2019) 245-250, https://doi.org/10.1016/j.inoche.2019.01.035
29. Adhikary, J., Majumdar, I., Kundu, P., Kornweitz, H., Kara, H., Das, D., ChemistrySelect, 3, (2018) 1445-1454, https://doi.org/10.1002/slct.201702861
30. Osório, R. E. H. M. B., Peralta, R. A., Bortoluzzi, A. J., Almeida, V. R., Szpoganicz, B., Fischer, F. L., Terenzi, H., Mangrich, A. S., Mantovani, K. M., Ferreira, D. E. C., Rocha, W. R., Haase, W., Tomkowicz, Z., Anjos, A., Neves, A., Inorg. Chem., 51, (2012) 1569-1589, https://doi.org/10.1021/ic201876k
31. Volkmer, D., Hommerich, B., Griesar, K., Haase, W., Krebs, B., Inorg. Chem, 35, (1996) 3792-3803, https://doi.org/10.1021/ic951567x
32. Barrios, A. M., Lippard, S. J., J. Am. Chem. Soc., 121, (1999) 11751-11757, https://doi.org/10.1021/ja992447h
33. Mazzei, L., Cianci, M., Benini, S., Bertini, L., Musiani, F. Ciurli, S., J. Inorg. Biochem., 154, (2016) 42-49, https://doi.org/10.1016/j.jinorgbio.2015.11.003

34. Carlsson, H., Haukka, M., Nordlander, E., Inorg. Chem., 41, (2002) 4981-4983, https://doi.org/10.1021/ic025839p
35. Carlsson, H., Haukka, M., Bousseksou, A., Latour, J., Nordlander, E., Inorg. Chem., 43, (2004) 8252-8262, https://doi.org/10.1021/ic049048u
36. Wages, H. E., Taft, K. L., Lippard, S. J., Inorg. Chem., 32, (1993) 4985-4987, https://doi.org/10.1021/ic00075a001
37. Chakraborty, T., Mukherjee, S., Dasgupta, S., Biswas, B., Das, D., Dalton Trans., 48, (2019) 2772-2784, https://doi.org/10.1039/c8dt04631j
38. Vichard, C., Kaden, T. A., Inorganica Chim. Acta, 337, (2002) 173-180, https://doi.org/10.1016/s0020-1693(02)00997-0
39. Horn Jr, A., Englert, D., Roberts, A. E., Comba, P., Schenk, G., Krenske, E. H., Gahan, L. R., Front. Chem., 6, (2018) 441, https://doi.org/10.3389/fchem.2018.00441
40. De Rosch, M. A., Togler, W. C., Inorg. Chem., 29, (1990) 2409-2416, https://doi.org/10.1021/ic00338a006
41. Mandal, S., Balamurugan, V., Lloret, F., Mukherjee, R., Inorg. Chem., 48, (2009) 7544-7556, https://doi.org/10.1021/ic8018937
42. Greatti, A., Scarpellini, M., Peralta, R. A., Casellato, A., Bortoluzzi, A. J., Xavier, F. R., Jovito, R., Brito, M. A., Szpoganicz, B., Tomkowicz, Z., Rams, M., Haase, W., Neves, A., Inorg. Chem., 47, (2008) 1107-1119, https://doi.org/10.1021/ic702132t
43. Piovezan, C., Silva, J. M. R., Neves, A., Bortoluzzi, J. A., Haase, W., Tomkowicz, Z., Castellano, E. E., Hough, T. C. S., Rossi, L. M., Inorg. Chem., 51, (2012) 6104-6115, https://doi.org/10.1021/ic300018t
44. Zeer-Wanklyn, C. J., Zamble, D. B., Curr. Op. Chem. Bio., 37, (2017) 80-88, https://doi.org/10.1016/j.cbpa.2017.01.014
45. Selleck, C., Clayton, D., Gahan, L. R., Mitić, N., McGeary, R. P., Pedroso, M. M., Guddat, L. W., Schenk, G., Chem. Eur. J., 23, (2017) 4778-4781, https://doi.org/10.1002/chem.201700866
46. Zhao, M., Xue, S. S., Jiang, X. Q., Zheng, L., Ji, L. N., J. Mol. Catal. A-Chem., 396, (2015) 346-352, https://doi.org/10.1016/j.molcata.2014.10.020
47. Pathak, C., Kumar, D., Gangwar, M. K., Mhatre, D., Roisnel, T., Ghosh, P., J. Inorg. Biochem., 185, (2018) 30-42, https://doi.org/10.1016/j.jinorgbio.2018.04.018

48. Bazzicalupi, C., Bencini, A., Bianchi, A., Fusi, V., Giorgi, C., Paoletti, P., Valtancoli, B., Zanchi, D., Inorg. Chem., 36, (1997) 2784-2790, https://doi.org/10.1021/ic961521j
49. Mahapatra, P., Drew, M. G. B., Ghosh, A., Inorg. Chem., 57, (2018) 8338-8353, https://doi.org/10.1021/acs.inorgchem.8b00995
50. Dalle, K. E., Meyer, F., Eur. J. Inorg. Chem., (2015) 3391-3405, https://doi.org/10.1002/ejic.201500185
51. Camargo, T. P., Neves, A., Peralta, R. A., Chaves, C., Maia, E. C. P., Jaimes, E. H. L., Gomes, D. A., Bortolotto, T., Norberto, D. R., Terenzi, H., Tierney, D. L., Schenk, G., Inorg. Chem., 57, (2018) 187-203, https://doi.org/10.1021/acs.inorgchem.7b02384
52. Saban, E., Chen, Y. H., Hangasky, J. A., Taabazuing, C. Y., Holmes, B. E., Knapp, M. J., Biochemistry, 50, (2011) 4733-4740, https://doi.org/10.1021/bi102042t
53. Ginovska-Pangovska, B., Dutta, A., Reback, M. L., Linehan, J. C., Shaw, W. J., Acc. Chem. Res., 47, (2014) 2621-2630, https://doi.org/10.1021/ar5001742
54. Bosch, S., Comba, P., Gahan, L. R., Schenk, G., Inorg. Chem., 53, (2014) 9036-9051, https://doi.org/10.1021/ic5009945
55. Cook, S. A., Borovik, A. S., Acc. Chem. Res., 48, (2015) 2407-2414, https://doi.org/10.1021/acs.accounts.5b00212
56. Zhao, M., Wang, H. B., Ji, L. N., Mao, Z. W., Chem. Soc. Rev., 42, (2013) 8360-8375, https://doi.org/10.1039/c3cs60162e
57. Mann, S. I., Heinisch, T., Ward, T. R., Borovik, A. S., Chem. Commun., 54, (2018) 4413-4416, https://doi.org/10.1039/c8cc01931b
58. Stone, E. M., Chantranupong, L., Georgiou G., Biochemistry, 49, (2010) 10582-10588, https://doi.org/10.1021/bi101542t
59. Gordon, Z., Drummond, M. J., Matson, E. M., Bogart, J. A., Schelter, E. J., Lord, R. L., Fout, A. R., Inorg. Chem., , https://doi.org/10.1021/acs.inorgchem.6b03071
60. Hadler, K. S., Mitić, N., Yip, S. H., Gahan, L. R., Ollis, D. L., Schenk, G., Larrabee, J. A., Inorg. Chem., 49, (2010) 2727-2734, https://doi.org/10.1021/ic901950c
61. Silva, G. A. S., Amorim, A. L., Souza, B., Gabriel, P., Terenzi, H., Nordlander, E., Neves, A., Peralta, R. A., Dalton Trans., 46, (2017) 11380-11394, https://doi.org/10.1039/c7dt02035j

62. Poornima, S., Gunasekaran, K., Kandaswamy, M., Dalton Trans., 44, (2015) 16361-16371, https://doi.org/10.1039/c4dt01744g
63. Liang, F., Wang, P., Zhou, X., Li, T., Li, Z., Lin, H., Gao, D., Zheng, C., Wu, C., Bioorg. Med. Chem. Lett., 14, (2004) 1901-1904, https://doi.org/10.1016/j.bmcl.2004.01.089
64. Zhong, X., Wei, H. L., Liu, W. S., Wang, D. Q., Wang, X., Bioorg. Med. Chem. Lett., 17, (2007) 3774-3777, https://doi.org/10.1016/j.bmcl.2007.04.006
65. Shrivastav, A., Singh, N. K., Singh, S. M., Bioorg. Med. Chem., 10, (2002) 887-895, https://doi.org/10.1016/s0968-0896(01)00373-x
66. Cui, Y., Wu, L., Yue, W., Lian, F., Qu, J., J. Mol. Struct., 1191, (2019) 145-151, https://doi.org/10.1016/j.molstruc.2019.04.081
67. Chohan, Z. H., Kausar, S., Met. Based Drugs, 7, (2000) 17-22, https://doi.org/10.1155/mbd.2000.17
68. Rao, N. K., Reddy, M. R., Biol. Met., 3, (1990) 19-23, https://doi.org/10.1007/bf01141172
69. Thirumalaikumar, M., Sivakolunthu, S., Muthusubramanian, S., Mohan, P., Sivasubramanian, S., 138, (1999) 107-210.
70. Chohan, Z. H., Pervez, H., Rauf, A., Scozzafava, A., Supuran, C. T., J. Enzyme Inhib. Med. Chem., 17, (2002) 117-122, https://doi.org/10.1080/14756360290024218
71. Singh, N. K., Singh, S. B., Singh, N., Shriviastav, A., Biometals, 16, (2003) 471-477, https://doi.org/10.1023/a:1022571817364
72. Patel, M .N., Patel, N. H., Panchal, P. K., Patel, D. H., Synth. React. Inorg. M., 34, (2004) 873-882, https://doi.org/10.1081/sim-120037513
73. Anacona, J. R., Salazar, R., Santaella, J., Celis, F., Inorg. Nano-Met. Chem., 48, (2018) 404-411, https://doi.org/10.1080/24701556.2019.1569681
74. Özdemir, Ü. Ö., Akkaya, N., Özbek, N., Inorganica Chim. Acta, 400, (2013) 13-19, https://doi.org/10.1016/j.ica.2013.01.031
75. Kulkarni, A., Avaji, P. G., Bagihalli, G. B., Patil, P. G., Badami, P. S., J. Coord. Chem., 62, (2009) 481-492, https://doi.org/10.1080/00958970802226387
76. Pereira, C., Farias, G., Maranha, F. G., Castilho, N., Schenk, G., Souza, B., Terenzi, H., Neves, A., Peralta, R. A., J. Biol. Inorg. Chem., 24, (2019) 675-691, https://doi.org/10.1007/s00775-019-01680-3

77. Karsten, P., Neves, A., Bortoluzzi, A. J., Lanznaster, M., Drago, V., Inorg. Chem., 41, (2002) 4624-4626, https://doi.org/10.1021/ic025674k
78. Bunton, C. A., Farber, S. J., J. Org. Chem., 34, (1969) 767-772, https://doi.org/10.1021/jo01256a001
79. Strohalm, M., Kavan, D., Novák, P., Volný, M., Havlíček, V., mMass 3: A Cross-Platform Software Environment for Precise Analysis of Mass Spectrometric data. Anal. Chem., 82, (2010) 4648-4651.
80. Gagné, R. R., Koval, C. A., Lisensky, G. C., Inorg. Chem., 19, (1980) 2854-2855, https://doi.org/10.1021/ic50211a080
81. Herrador, M. A., González, A. G., Talanta, 56, (2002) 769-775, https://doi.org/10.1016/s0039-9140(01)00607-5
82. Martell, A. E., Motekaitis, R. J., Determination and use of stability constants, VCH publishers, 1992.
83. Peralta, R. A., Bortoluzzi, J. A., Souza, B., Jovito, R., Xavier, F. R., Couto, R. A. A., Caselatto, A., Nome, F., Dick, A., Gahan, L. R., Schenk, G., Hanson, G. R., Paula, F. C. S., Pereira-Maia, E. C., Machado, S. P., Severino, P. C., Pich, C., Bortolotto, T., Terenzi, H., Castellano, E. E., Neves, A., Riley, M. J., Inorg. Chem., 49, (2010) 11421-11438, https://doi.org/10.1021/ic101433t
84. Berg, J. M., Tymoczko, J. L., Stryer, L., Biochemistry, W.H. 2002.
85. Wayne, P. A., Clinical and laboratory standards institute (CLSI) M07-A10. Methods for dilution antimicrobial susceptibility tests for bacteria that grow aerobically; approved standard-tenth edition, 2015.
86. Neese, F., Software update: the ORCA program system, version 4.0. Wiley Interdisciplinary Reviews: Computational Molecular Science,8, (2017), e1327, https://doi.org/10.1002/wcms.1327
87. Becke, A. D., Phys. Rev. A, 38, (1988) 3098–3100, https://doi.org/10.1103/PhysRevA.38.3098
88. Perdew, J. P. Phys. Rev. B, 33, (1986) 8822–8824, https://doi.org/10.1103/PhysRevB.33.8822
89. Schäfer, A., Horn, H., Ahlrichs, R., J. Chem. Phys, 97, (1992) 2571, https://doi.org/10.1063/1.463096

90. Schäfer, A., Huber, C., Ahlrichs, R., J. Chem. Phys., 100, (1994) 5829, https://doi.org/10.1063/1.467146
91. Weigend, F., Ahlrichs, R., Phys. Chem. Chem. Phys., 7, (2005), 3297-3305, https://doi.org/10.1039/b508541a
92. Grimme, S., Antony, J., Ehrlrich, S., Krieg, H., J. Chem. Phys., 132, (2010) 154104, https://doi.org/10.1063/1.3382344
93. Grimme, S., Ehrlrich, S., Goerigk, J. Comput. Chem., 32, (2011) 1456-1465, https://doi.org/10.1002/jcc.21759
94. Perdew, J. P., Burke, K., Ernzerhof, M., Phys. Rev. Lett., 77, (1996) 3865-3868, https://doi.org/10.1103/PhysRevLett.77.3865
95. Perdew, J. P., Burke, K., Ernzerhof, M., Phys. Rev. Lett., 78, (1997) 1396, https://doi.org/10.1103/PhysRevLett.78.1396
96. www.chemcraftprog.com
97. Nakamoto, K., Infrared and raman spectra of inorganic and coordination compounds. Wiley, 1977.
98. Tanabe, Y., Sugano, S., J. Phys. Soc. Jpn., 9, (1954) 766-779, https://doi.org/10.1143/jpsj.9.766
99. Anbu, S., Kandaswamy, M., Suthakaran, P., Murugan, V., Varghese, B., J. Inorg. Biochem., 103, (2009) 401-410, https://doi.org/10.1016/j.jinorgbio.2008.12.013
100. Geary, W. J., Coord. Chem. Rev., 7, (1971) 81-122, https://doi.org/10.1016/s0010-8545(00)80009-0
101. Batista, S. C., Neves, A., Bortoluzzi, A. J., Vencato, I., Peralta, R. A., Szpoganicz, B., Aires, V. V. E., Terenzi, H., Severino, P. C., Inorg. Chem. Commun., 6, (2003) 1161-1165, https://doi.org/10.1016/s1387-7003(03)00219-3
102. Lanznaster, M., Neves, A., Bortoluzzi, A. J., Szpoganicz, B., Schwingel, E., Inorg. Chem., 41, (2002) 5641-5643, https://doi.org/10.1021/ic025892d
103. Lambert, E., Chabut, B., Chardon-Noblat, S., Deronzier, A., Chottard, G., Bousseksou, A., Tuchagues, J. P., Laugier, J., Bardet, M., Latour, J. M., J. Am. Chem. Soc., 119, (1997) 9424-9437, https://doi.org/10.1021/ja970345q
104. Barman, S. K., Lloret, F., Mukherjee, R., Inorg. Chem., 55, (2016) 12696-12706, https://doi.org/10.1021/acs.inorgchem.6b01895

105. Cox, B. G., Acids and bases: solvent effects on acid-base strength. OUP Oxford, 2013.
106. Piszkiewicz, D., Kinetics of Chemical and Enzyme-Catalyzed Reactions. Oxford University Press: New York, 1977, pp 81-106
107. Massoud, S. S., Ledet, C. C., Junk, T., Bosch, S., Comba, P., Herchel, R., Hošek, J., Trávníček, Z., Fischer,R. C., Mautner, F. A., Dalton. Trans., 45, (2016) 12933-12950, https://doi.org/10.1039/c6dt02596j
108. Jarenmark, M., Haukka, M., Demeshko, S., Tuczek, F., Zuppiroli, L., Meyer, F., Nordlander, E., Inorg. Chem., 50, (2011) 3866-3887, https://doi.org/10.1021/ic1020324
109. Muxel, A. A., Neves, A., Camargo, M. A., Bortoluzzi, A. J., Szpoganicz, B., Castellano, E. E., Castilho, N., Bortolotto, T., Terenzi, H., Inorg. Chem., 53, (2014) 2943-2952, https://doi.org/10.1021/ic402705r
110. Deal, K. A., Hengge, A. C., Burstyn, J. N., J. Am. Chem. Soc., 118, (1996) 1713-1718, https://doi.org/10.1021/ja952306p
111. Wilkins, R. G., Kinetics and Mechanism of Reactions of Transition Metal Complexes. 2nd ed: VCH: Weinheim, 1991.
112. Kirby, A. J., Younas, M., J. Chem. Soc. B., (1970) 1165-1172, https://doi.org/10.1039/j29700001165
113. Cui, P., Wang, Y., Chu, W., Guo, X., Yang, F., Yu, M., Zhao, H., Dong, Y., Xie, Y., Gong, W., Wu, Z., Sci. Rep., 4(7453) (2015), https://doi.org/10.1038/srep07453
114. Gomathi, V., Selvameena, R., Inorganica Chim. Acta, 480, (2018) 42-46, https://doi.org/10.1016/j.ica.2018.05.007
115. Galini, M., Salehi, M., Kubicki, M., Amiri, A., Khaleghian, A., Inorganica Chim. Acta, 461, (2017) 167-173, https://doi.org/10.1016/j.ica.2017.02.001
116. Salehi, M., Rahimifar, F., Kubicki, M., Asadi, A., Inorganica Chim. Acta, 443, (2016) 28-35, https://doi.org/10.1016/j.ica.2015.12.016
117. Özdemir, Ü. Ö., Güvenç, P., Şahin, E., Hamurcu, F., Inorganica Chim. Acta, 362, (2009) 2613-2618, https://doi.org/10.1016/j.ica.2008.11.029

- Three new Ni(II) complexes with amine pendant ligands were synthesized.
- All complexes were characterized by several techniques including DFT method.
- Hydrolase-like and antibacterial activities for all complexes were investigated.
- **2** showed significant antibacterial activity towards all bacteria strains tested.